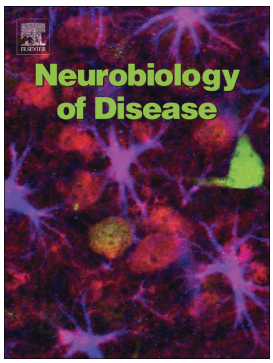

Human amyloid β peptide and tau co-expression impairs behavior and causes specific gene expression changes in Caenorhabditis elegans

Chenyin Wang, Valeria Saar, Ka Lai Leung, Liang Chen, Garry Wong

PII: S0969-9961(17)30220-6
DOI: doi:10.1016/j.nbd.2017.10.003
Reference: YNBDI 4042

To appear in: *Neurobiology of Disease*

Received date: 17 May 2017
Revised date: 11 September 2017
Accepted date: 1 October 2017

Please cite this article as: Chenyin Wang, Valeria Saar, Ka Lai Leung, Liang Chen, Garry Wong , Human amyloid β peptide and tau co-expression impairs behavior and causes specific gene expression changes in Caenorhabditis elegans. The address for the corresponding author was captured as affiliation for all authors. Please check if appropriate. Ynbdi(2017), doi:10.1016/j.nbd.2017.10.003

Human Amyloid β peptide and tau co-expression impairs behavior and causes specific gene expression changes in *Caenorhabditis elegans*

Chenyin Wang, Valeria Saar, Ka Lai Leung, Liang Chen, Garry Wong*

Faculty of Health Sciences, University of Macau, Macau S.A.R., China 999078

*To Whom Correspondence should be addressed:

Prof. Garry Wong

Faculty of Health Sciences

Avenida da Universidade

University of Macau

Macau S.A.R. CHINA

999078

TEL: +853 8822 4979; FAX: +853 8822 2314

EMAIL: GarryGWong@umac.mo

Abstract

Alzheimer's disease (AD) is a progressive neurodegenerative disorder characterized by the presence of extracellular amyloid plaques consisting of Amyloid-β peptide (Aβ) aggregates and neurofibrillary tangles formed by aggregation of hyperphosphorylated microtubule-associated protein tau. We generated a novel invertebrate model of AD by crossing Aβ1-42 (strain CL2355) with either pro-aggregating tau (strain BR5270) or anti-aggregating tau (strain BR5271) pan-neuronal expressing transgenic *Caenorhabditis elegans*. The lifespan and progeny viability of the double transgenic strains were significantly decreased compared with wild type N2 (P<0.0001). In addition, co-expression of these transgenes interfered with neurotransmitter signaling pathways, caused deficits in chemotaxis associative learning, increased protein aggregation visualized by Congo red staining, and increased neuronal loss. Global transcriptomic RNA-seq analysis revealed 438 up- and 797 down-regulated genes in N2 wild type versus Aβ1-42 + pro-aggregating tau animals, compared to 36 up- and 46 down-regulated genes in N2 wild type versus Aβ1-42 + anti-aggregating tau animals. Gene set enrichment analysis of Aβ1-42 + pro-aggregating tau animals uncovered up-regulated annotation clusters UDP-glucuronosyltransferase (5 genes, P<4.2E-4), protein phosphorylation (5 genes, P<2.60E-02), and aging (5 genes, P<8.1E-2) while the down-regulated clusters included nematode cuticle collagen (36 genes, P<1.5E-21).

RNA interference of 13 available top up-regulated genes in Aβ1-42 + pro-aggregating tau animals revealed that F-box family genes and *nep-4* could enhance life span deficits and chemotaxis deficits while Y39G8C.2 (TTBK2) could suppress these behaviors.

Comparing the list of regulated genes from *C. elegans* to the top 60 genes related to human AD confirmed an overlap of 8 genes: patched homolog 1, PTCH1 (*ptc-3*), the Rab GTPase activating protein, TBC1D16 (*tbc-16*),the WD repeat and FYVE domain-containing protein 3, WDFY3 (wdfy-3), ADP-ribosylation factor guanine nucleotide exchange factor 2, ARFGEF2 (*agef-1*), Early B-cell Factor, EBF1 (*unc-3*),

D-amino-acid oxidase, DAO (*daao-1*), glutamate receptor, metabotropic 1, GRM1 (*mgl-2*), prolyl 4-hydroxylase subunit alpha 2, P4HA2 (*dpy-18* and *phy-2*). Taken together, our *C. elegans* double transgenic model provides insight on the fundamental neurobiologic processes underlying human AD and recapitulates selected transcriptomic changes observed in human AD brains.

Abbreviations

AD, Alzheimer's disease; Aβ, Amyloid-β peptide; PTCH1, patched homolog 1; TBC1D16, the Rab GTPase activating protein; WDFY3, the WD repeat and FYVE domain-containing protein 3; ARFGEF2, ADP-ribosylation factor guanine nucleotide exchange factor 2; EBF1, Early B-cell Factor; DAO, D-amino-acid oxidase; GRM1, glutamate receptor, metabotropic 1; P4HA2, prolyl 4-hydroxylase subunit alpha 2; APP, Amyloid precursor protein; MAPT, microtubule-associated protein; FUdR, 5-fluorodeoxyuridine; DAVID, Database for Annotation, Visualization and Integrated Discovery; GO, Gene Ontology

Keywords

Caenorhabditis elegans; Alzheimer's disease; transcriptome analysis; Amyloid beta; tau; RNA interference

1. Introduction

Transgenic models of neurodegenerative diseases have been invaluable for the study of molecular mechanisms, etiology, as well as development and testing of therapies. For investigations in Alzheimer's disease (AD), transgenic models in mice and roundworms have been developed and have contributed immensely to our understanding of the neurobiology and pathophysiology of this disease (Lewis et al., 2001; Link, 1995). In these models, overexpressed transgenes include human versions of amyloid beta (Aβ) and tau while mutant versions include presenillin. These transgenic models could recapitulate some aspects of AD including the presence of aggregated proteins in extracellular plaques and intraneuronal neurofibrillary tangles (NFT) consisting of Aβ and tau, respectively.

Amyloid β-peptide (Aβ) is a 38 to 42 amino acid peptide which is a cleavage product of Amyloid precursor protein (APP), a transmembrane protein. If APP is first cut by α-secretase then γ-secretase sequentially, it will generate a large N-terminal peptide called soluble APPα and a 3kD peptide P3. This process is termed the non-amyloidogenic pathway. But, if APP is first cleaved by β- secretase and then the γ-secretase complex, the C-terminal membrane-bound fragment is liberated, thus making Aβ peptides i.e., $Aβ_{1-40}$ and $Aβ_{1-42}$. Aβ peptides aggregate to plaques extracellularly and prevents neurotransmission from pre- to post-synaptic cells, eventually leading to synaptic dysfunction and neuronal cell death (Ittner &Götz, 2011). Mutations in the genes encoding APP and γ-secretase complex (presenilin 1 and presenilin 2) have been identified as the genetic risk factors of early-onset AD (St George-Hyslop et al., 1992; Goate et al., 1991; Levy-Lahad et al., 1995).

Another AD associated gene, tau, is composed of hyperphosphorylated forms of the microtubule-associated protein (MAPT). In diseased neurons, aberrantly hyperphosphorylated tau reduces its affinity to bind microtubules and self-aggregates into NFTs, which disrupt the structure and function of the neuron. Mutations in frontotemporal dementia and parkinsonism linked to chromosome 17 type (FTDP-17), the gene encoding tau can alter function and level of tau and cause

dementia (Hutton et al., 1998; Foster et al., 1997).

Findings from transgenic mammalian studies have provided significant insight into this disorder, however, the fundamental mechanism of proteotoxicity involved in the pathogenesis of AD remain unclear. The first double transgenic mice model of AD was generated by crossing JNPL3 mice (the P301L tau mutation) with Tg2576 (the APPsw mutation) (Lewis et al., 2001). It revealed an interaction between APP or Aβ and tau that leads to increased NFT formation and distribution in regions of brain vulnerable to these lesions. The same phenomena was observed by crossing JNPL3 mice with another APP transgenic mouse model, APP23, showing that the resulting double transgenic mice develop exacerbated tau pathology in areas with high Aβ plaques (Bolmont et al., 2007).

As one of the widely used model organisms, *Caenorhabditis elegans* has been important in furthering our understanding of the mechanisms of many forms of neurodegenerative diseases, including AD (Li et al., 2013; Martorell et al., 2013; Alexander et al., 2014; Smialowska et al., 2006; Kraemer et al., 2003). Transgenic *C. elegans* models ectopically overexpress the human Aβ or tau individually have previously been produced (Link, 1995; Fatouros et al., 2012; Wu et al., 2006; McColl et al., 2012; Brandt et al., 2009). These animals have made important contributions to the understanding of AD, including anti-Aβ/tau based drug screening and testing (Sangha et al., 2012; Martorell et al., 2013; Dostal et al., 2010), identification of the molecular mechanisms underlying the action of protective compounds (Xin et al., 2013) and revelation of etiology and pathogenesis of AD (Sonani and Singh, 2014; Kraemer et al., 2006). While these single transgenic animals have been powerful, a significant improvement would a nematode model expressing both Aβ and tau transgenes.

In this study, we generated a new *C. elegans* model by co-expression of Aβ and tau in pan-neuronal cells. The model recapitulates many of the pathologies observed in human AD, including synaptic fatigue (Schroeder et al., 2005; Zhao et al., 2010),

cognitive aging (Ballard et al., 2011), and shorter longevity (Larson et al., 2004). We extended these observations by verifying the differences in transcriptome profiles between human AD brain and our *C. elegans* model. Our results suggest a novel *C. elegans* model that can be used to reveal the pathogenesis of human AD and to identify potential neuroprotective genes that can increase our understanding of tau- and Aβ-mediated neurotoxicity.

2. Materials and Methods

2.1 *C. elegans* strains and maintenance

Animals were cultivated on nematode growth medium (NGM) plates on the *Escherichia coli* strain OP50 by standard methods (Brenner, 1974).

2.2 Genetic crosses

UM0001 was generated by crossing strains CL2355 (Wu et al., 2006) and BR5270 (Fatouros et al., 2012), and UM0002 was generated by crossing CL2355 and BR5271 (Fatouros et al., 2012). Briefly, N2 males were mated with CL2355 [P_{snb-1}::$A\beta_{1-42}$; P_{mtl-2}::GFP] hermaphrodites and the resulting transgenic male offspring were then crossed to BR5270 [P_{rab-3}::F3(delta)K280; P_{myo-2}::mCherry] or [BR5271 P_{rab-3}::F3(delta)K280 I277P I380P; P_{myo-2}::mCherry] hermaphrodites. The progenies with both GFP and mCherry markers were checked under the fluorescence microscopy for heterozygotes, and after singling these animals, homozygotes were identified. To verify homozygosity of both transgenes, the animals were genotyped via single-worm PCR using primers: human *MAPT* tau forward: 5'- ATG GCT GAG CCC CGC CAG GAG TTC-3'; reverse: 5'- TCA CAA ACC CTG CTT GGC CAG-3', human Aβ forward: 5'- GAT GCA GAA TTC CGA CAT GA-3'; reverse: 5'- ACG CTA TGA CAA CAC CGC CAA-3'. The list of strains used and their genotype and phenotype are shown in **Table 1**.

2.3 Lifespan assay

The assay was performed according to *He et al* (2011) with a few modifications. Fifty age-synchronized worms were maintained in NGM plates at 16°C until they reached the L4 stage. Ten L4s were transferred to NGM plate (60×15 mm), which contained

50 µg/mL 5-fluorodeoxyuridine (FUdR) (Sigma-Aldrich, USA). Five replicates were made for each strain. The animals were cultivated at 23°C and the mortality rate was scored every two days by gentle prodding of the anterior end of the body with a platinum wire.

2.4 Egg laying assay

Age-synchronized animals were maintained on NGM plates at 16°C with OP50 from embryos until they reached the L4 stage. Animals were subjected to heat shock at 23°C overnight (16 h). Two worms were transferred per well of a 96-well plate containing 100 µL of M9 buffer, 5 mg/mL solution of serotonin, or 10 mg/mL of levamisole. The number of groups per treatment was 32. The number of eggs released from each worm at room temperature was scored after 1 hour. For reproductive life span assays,

Age-synchronized animals were maintained on NGM plates at 16°C with OP50 from embryos until they reached the L4 stage. The animals were transferred to 12 well plates, one worm/well. Eggs were measured after 24h and adult animals were transferred every day to new plates until the end of the assay.

2.5 Progeny viability assay

Age-synchronized animals were maintained in NGM plates at 16°C from embryos until they reached the L4 stage. Animals were subjected to heat shock at 23°C overnight (16 h). Two one day old young adults were transferred per well on 12-well plates. Animals were cultivated at 23°C until ~20 eggs were laid. The number of animals assayed per strain was 24. The adults were removed and the number of hatched L1 worms were counted the following day. The percentage viability = (L1 worms/ number of eggs) × 100%.

2.6 Basal slowing response assay

The assay was performed according to *Sawin et al.* (2000) with minor modifications. Synchronized embryos were cultivated in NGM plates with E. coli strain OP 50 at 16°C until they reached the L4 stage. Animals were subjected to heat shock at 23°C overnight (16 h). Only well-fed synchronized young adults were tested. To prevent

bias, plates were coded so that the experimenter was blind to the genotype. The locomotion rate was measured on a bacteria free plate by calculating the worm's body bends in 20 seconds. To avoid over-stimulation of worm activity, counting was started 5 minutes after transfer.

2.7 Chemotaxis assay associated with learning

Learning ability was measured by odorant preference assay described by *Kauffman et al*(2011) with a few modifications. Briefly, age-synchronized animals were maintained in NGM plates at 16°C from embryos to L4 stage. The temperature was up-shifted to 23°C overnight. Well-fed young adults were collected with M9 and washed 3 times to remove bacteria (settled by gravity). Synchronized worms were harvested and divided into naive, trained and control groups. Each group was performed in triplicate and contained about 200-400 worms. The rest of the worms were starved in the M9 for 1 hour. In the naive group, the washed worms were placed directly onto assay plates. For the trained group, worms were then transferred to NGM plates containing OP50 bacteria, and 2 µL of 10% butanone was added on the lid for odor training for 1 hour. After one hour, these two plates of worms were washed with M9. Worms in trained group were then washed off from the plates with M9 buffer and collected in tubes respectively. Worms were then transferred to assay plates for observation. The number of worms was counted on both butanone and ethanol spots containing sodium azide (1 µL of 1 M solution) after 1h. Chemotaxis index (CI) and Learning index (LI) were calculated as Chemotaxis index (CI): $[n_{but}-n_{eth}]/ [Total - n_{origin}]$; Learning Index (LI): $CI_{but} - CI_{naive}$.

2.8 Congo red staining

Fifty to one-hundred transgenic animals were transferred to a 2.5 µL drop of H_2O in a 14-mm circle on a microscope slide, compressed with a coverslip, and quick-frozen at -80°C. The coverslip was cracked off with a scalpel, and the frozen animals were repeatedly sliced with a scalpel. The cleaved animals were then quickly dried onto the slide by incubation on a 55°C heating block (~30 s), and a 25 µL drop of 0.5% Congo red (Sigma) in 50% ethanol/10 mM Tris (pH 7.5) was added. After a 3 h

incubation in a humid chamber at 20°C, the staining solution was removed by immersion in H_2O, and a fresh 25 µL drop of destaining solution (0.5% potassium hydroxide and 80% ethanol) was placed on the slide. Destaining was monitored under the dissecting microscope and the slide was immersed in H_2O as soon as dark red precipitates were observed (~40 s). A second drop of destain was added, and after 10 s the slide was again washed in H_2O. Immediately after drying, a 5 µL drop of mounting medium and a coverslip were added. Slides were observed with a Zeiss Axio Observer microscope at 400X magnification (excitation at 540 nm, emission at 477 nm).

2.9 Visualization of dopaminergic neurons

The triple transgenic animals were generated by crossing double transgenic animals UM0001 with P*dat-1*::GFP animals (Lakso et al., 2003). A total of 30 young adults were mounted on agarose pads and paralyzed with 1M sodium azide solution. The micrographs of dopaminergic neuron were taken by Zeiss confocal microscope LSM710 at 400X magnification. Imaging software used was ZEN (Zeiss, Jena, Germany).

2.10 RNA isolation and sequencing

Age-synchronized embryos were maintained on NGM plates seeded with bacteria strain NA22 at 16°C until L3 stage, the incubation temperature was up-shifted to 23°C until they reached the L4 stage. The L4s were washed with M9 buffer twice, and with sterile water once. Total RNA was isolated by TRIzol (Thermo Fisher Scientific, Waltham, Massachusetts, USA). RNA concentration was quantified using Nanodrop 2000c (Thermo Fisher Scientific,Waltham, Massachusetts, USA) and purified by RNeasy Mini kit (Qiagen, Hilden, Germany). RNA libraries were prepared according to the NEBNext® Ultra™ Directional RNA Library Prep Kit for Illumina (New England Biolabs, Ipswich, Massachusetts, USA). The libraries were sequenced in duplicate on the Illumina Hiseq 2000 at the Genomics and Bioinformatics Core in the Faculty of Health Sciences, University of Macau (Macau, China).

Reads were aligned to the *C. elegans* genome (WS220) using software TopHat

implementation 2.0.13 of Bowtie 2.2.4.0 (Trapnell et al., 2009). To identify differential gene expression, analysis was performed using Cuffdiff program of Cufflinks 2.2.1 with false discovery rate–corrected p values (q values) of <0.05 and log2 (fold change) >1 or <-1. Gene enrichment analysis was performed for up- and down-regulated genes using Database for Annotation, Visualization and Integrated Discovery (DAVID) Functional Annotation Tool 6.7 (Huang et al., 2009b; Huang et al., 2009a). The biological function represented by Gene Ontology terms with a Benjamini–Hochberg (BH) corrected *P* value <0.05 were deemed significant. Heatmaps were generated using the significant genes in the comparison between wild type N2 and transgenic strain fold change >3 as cut off. The double transgenic *C. elegans* model was also compared to a previously published data set from human AD brain tissue (Twine et al., 2011) to identify differentially expressed genes associated with AD pathogenesis.

2.11 Quantitative Real-Time PCR (qRT-PCR)

Based on RNA-seq data, four genes (*ptc-3, wdfy-3, agef-1, mgl-2*) that overlapped with human AD brain were selected for verification using qRT-PCR. The age-synchronized embryos of N2, CL2355, BR5270, BR5271, UM0001 and UM0002 strains were synchronized and maintained at 16°C until L3 stage. The incubation temperature was then up-shifted to 23°C until they reached the L4 stage. Total RNA from L4 animals was isolated and purified as described above. Two micrograms of total RNA were used for the reverse transcription reaction. Amplification was detected using SYBR Green (BioRad, Hercules, California, USA) using the Real-Time PCR System CFX96 (BioRad, Hercules, California, USA). Each of 4 biological replicates was performed in duplicate technical replicates. Gene expression differences were calculated using the ΔΔCt method (Livak et al., 2001). The housekeeping gene *act-1* was used as an internal control. This gene has been used previously as the internal control for qRT-PCR experiments (Rudgalvyte et al., 2015).

2.12 RNA interference

The double transgenic strain UM0001 which co-expresses human Aβ and tau was

crossed with a neuronal RNAi sensitizing strain TU3311 [*unc-119p*::YFP + *unc-119p*::*sid-1*] to enhance the neuronal RNAi sensitivity. RNA-mediated interference (RNAi) was performed on NGM plates containing 1mM Isopropyl β-D-1-thiogalactopyranoside (IPTG) and 100 μg/ml ampicillin. Plates were seeded with HT115 bacteria as a control (Addgene, Cambridge, MA). Bacteria cultures were grown for 10 h in liquid medium with each gene fragment (Source BioScience LifeSciences, Nottingham, UK) or empty vector supplemented with 100 μg/ml ampicillin and without IPTG at 37°C. After 10 h IPTG (1mM) was added, cultures were grown 4 h more and transferred onto plates. Embryos were transferred onto RNAi plates and left to grow until the appropriate stage for the phenotypic assay. Thirteen clones were available from the list of top 20 regulated genes.

2.13 Statistical analysis

Data presented in this article is shown in mean± S.E.M. One-way ANOVA, followed by a Tukey HSD post-hoc test was used for comparison between genotype strains and two-tailed student's *t*-test was used to compare between two groups. Differences were considered significant at $P< 0.05$. All statistical analysis was carried out by using GraphPad Prism 6.0 software (GraphPad Software, San Diego, CA, USA).

3 Results

3.1 Pan-neuronal Aβ and tau expression shorten the life span of *C. elegans*

Lifespan assay was performed to examine the aging process among wild type, single and double transgenic animals. Since the expression of Aβ in CL2355 is under control of a temperature-sensitive mRNA surveillance system that allows for up-regulation of Aβ peptide after heat shock (Wu et al., 2006), animals were incubated on NGM plates with 50 μg/mL FUdR at 23℃ after they reached the L4 stage. We observed that all the transgenic strains live significantly shorter than wild type animals (One-way ANOVA, $P<0.0001$). The double transgenic strain UM0001, which expresses both Aβ and pro-aggregating tau, has a shorter life span than the corresponding single transgenic strains CL2355 expressing Aβ or BR5270 expressing pro-aggregating

tau (P<0.0001) (**Fig. 1A, B**). Compared with UM0002 that expresses both Aβ and anti-aggregating tau, BR5271 that expresses anti-aggregating tau only, has a shorter life span (P<0.0001), but CL2355 does not, indicating that Aβ aggregates can shorten the life span, but anti-aggregating tau cannot.

3.2 Pan-neuronal Aβ and tau expression cause significantly decreased progeny viability.

To determine effects of transgenes on development, we performed progeny viability assays on single and double transgenic animals (**Fig.1C**). The progeny viability of anti-aggregating tau was essentially the same as wild type. The other transgenic strains CL2355 (Aβ1-42), BR5270 (pro-aggregating tau), UM0001 (Aβ1-42 + pro-aggregating tau) and UM0002 (Aβ1-42 + anti-aggregating tau), have significantly less progeny than wild type (P<0.01), suggesting that Aβ and pro-aggregating tau may affect developmental processes. Reproductive aging was also observed as CL2355 (Aβ1-42), BR5270 (pro-aggregating tau), and UM0001 (Aβ1-42 + pro-aggregating tau) strains produced nearly no progeny on day 4 while wild type and anti-aggregating tau strains were still producing (P<0.001) **(Fig. 1D).**

3.3 Pan-neuronal expression of Aβ disrupts chemotaxis associative learning, but not tau.

We tested the associative learning capacity of double transgenic *C. elegans* in an assay pairing butanone with food. We observed no significant difference between the pro-aggregating and anti-aggregating tau strains (**Fig. 1E**). However, the learning indexes of Aβ only and double transgenic strains containing Aβ + pro-aggregating tau or Aβ + anti-aggregating tau were significantly smaller (P<0.01) than wild type N2 strain. These deficits also increased as animals aged as Aβ, Aβ + pro-aggregating tau, and Aβ + anti-aggregating tau animals performance declined in chemotaxis to learning index negative values **(Fig. 1F).**

3.4 Pan-neuronal expression of Aβ and tau interferes with egg laying in *C. elegans*

Transgenic animals expressing Aβ, pro-aggregating tau, or the two in combination, laid significantly fewer eggs than wild type when stimulated with serotonin (P<0.0001) (**Fig. 2A**). The anti-aggregating tau animals were not significantly different than wild type. When the double transgenic animals expressing both Aβ and pro-aggregating tau were compared to single transgenic Aβ, the latter laid significantly more eggs (P<0.0001) but not compared to pro-aggregating tau, suggesting that pro-aggregating tau severely impairs egg-laying in the presence of Aβ. We questioned whether anti-aggregating tau plays the same function as pro-aggregating tau. However, there is no significant difference between single transgenic Aβ and double transgenic Aβ + anti-aggregating tau, suggesting that only the pro- aggregated tau impairs egg laying.

To test whether Aβ and tau affect cholinergic signaling, we also treated worms with levamisole (10 mg/mL), an agonist of acetylcholine receptors (AChRs), which should also increase egg laying (**Fig.2A**). The results showed an insignificant change of egg laying between transgenic Aβ and wild type, consistent with previous research (Dosanjh et al., 2010). Compared with wild type, pro-aggregating tau, pro-aggregating tau + Aβ, anti-aggregating tau + Aβ laid significantly fewer eggs (P<0.0001). Compared to Aβ only (CL2355), Aβ + pro-aggregating tau (UM0001), and Aβ + anti-aggregating tau (UM0002) showed a significant difference (P<0.0001), indicating that both pro-aggregating tau and anti-aggregating tau severely impair cholinergic signaling. Taken together, the aggregated tau impaired serotoninergic and cholinergic signaling with or without the presence of Aβ. Aβ appears to impair serotoninergic but not cholinergic signaling in an egg laying behavior. In the presence of both pro-aggregating tau and anti-aggregating tau, Aβ aggregates did not impair cholinergic signaling (P>0.05). Anti-aggregating tau did not impair serotoninergic and cholinergic signaling, but in the presence of Aβ, it severely impaired cholinergic signaling (P<0.0001).

Basal slowing response was assayed to determine transgene effects on dopaminergic signaling (Sawin et al., 2000) (**Fig.2B**). In the presence of bacteria, the

locomotory rate of well-fed *cat-1* and *cat-2* mutants on bacteria were significantly faster (***P<0.0001, Student's t-test) than that of well-fed wild type animals, which is consistent with the previous findings (Sawin et al., 2000). The single transgenic strains CL2355 (Aβ), BR5270 (pro-aggregating tau), BR5271 (anti-aggregating tau) and double transgenic strain UM0002 (Aβ+anti-aggregating tau) show a basal slowing response. However, the locomotion rate of UM0001 (Aβ+pro-aggregating tau) does not show a basal slowing response. Taken together, the results of basal slowing response assay indicate the co-expression of Aβ and pro-aggregating tau can impair dopaminergic signaling.

3.5 Congo red staining reveals aggregated proteins in Aβ + pro-aggregating tau double transgenic animals

The cellular localization of the accumulated transgenic Aß1-42 and tau was examined via Congo red staining. Congo red dye can bind to beta sheet-rich structure, like senile plaques (SP) and neurofibrillary tangles (NFT) (Wu et al, 2012). In **Fig. 3**, double transgenic animals (UM0001) expressing both Aβ and pro-aggregating tau appear to have extensively aggregated deposits stained positive for the Congo red **(Fig.3E)**. But in the pro-aggregating tau strain (BR5270), we observed fewer deposits than double transgenic strain (UM0001) **(Fig. 3B)**. We did not observe any deposits in the other strains wild type (N2), anti-aggregating tau strain (BR5271), Aβ1-42 strain (CL2355) and Aβ1-42+ anti-aggregating tau strain (UM0002), indicating that the co-existence of Aβ1-42 and pro-aggregating tau may be the initiator of protein aggregation **(Fig. 3A, C, D, F).**

3.6 Loss of dopaminergic neurons and punctate process pattern in Aβ + pro-aggregating tau double transgenic animals.

We observed loss of both CEP and ADE dopaminergic neurons in Aβ + pro-aggregating tau animals double transgenic animals **(Fig. 4)**. The loss was observed in 15/30 animals assayed. We also observed punctate expression pattern in

neuronal processes in 17/30 animals and both neuronal loss and punctate patterns in 8/30 while none of these deficits were observed in the GFP expressing control **(Fig. 4D)**.

3.7 RNA-seq reveals clustering of wild type, Aβ, pro-aggregating tau, and anti-aggregating animals

RNA-seq revealed 489 genes that were significantly regulated (3 fold change, $p<0.05$) between the 6 strains used in this study. A full list of FPKM values for all strains and all genes are found in **Supplementary Table 1**. The list for 489 genes regulated and used for clustering are found in **Supplementary Table 2.** Hierarchical clustering of these genes using Euclidean distance and average linkage for clustering revealed 3 pairs that clustered together: N2 wild type and anti-aggregating tau; Aβ and Aβ+anti-aggregating tau; and pro-aggregating tau + Aβ and pro-aggregating tau (**Fig.5**). We also performed hierarchical clustering using all genes with an expression value >0 consisting of 20467 genes and obtained similar results with the 3 pairs (**Supplementary Figure 1A**). Correlation analysis with the 20467 genes also showed clustering of wild type with anti-aggregating tau, Aβ animals together, and pro-aggregating tau the furthest (**Supplementary Figure 1B**).

3.8. Overlapping up- and down-regulated genes were identified

A list of significantly up- and down-regulated genes obtained from RNA-seq cuffdiff was obtained. Volcano plots of the genes found are shown in **Supplementary Figure 1C.** A list of the 15 most up- and down-regulated genes in N2 versus Aβ + pro-aggregating tau is shown in **Table 2**. A complete list of this comparison can be found in **Supplementary Table 3**. When comparisons were made between the 6 strains used in this study, hundreds of genes were found to be differentially expressed. Venn diagrams of up- and down-regulated genes show limited overlap of genes regulated by Aβ (**Fig. 6A, B**) suggesting that tau, whether pro- or anti-aggregating plays a role larger role in gene expression changes than Aβ. A large overlap was found in Aβ animals with either a wild type or anti-aggregating tau

background (79 genes up, 146 genes down) (**Fig. 6A, B**). A large number of genes were found regulated (1435 genes up, 1213 genes down) in Aβ animals alone versus Aβ +pro-aggregating tau (**Fig. 6C, D**). A large proportion (82 genes up, 481 down) of these were also regulated in pro-aggregating tau animals when compared to pro-aggregating tau animals alone **(Fig. 6C, D)**. Fewer genes were found to be regulated in Aβ alone versus Aβ + anti-aggregating tau (535 genes up, 171 genes down) (**Fig. 6E, F**). A very small number of genes were found regulated in anti-aggregating tau animals compared to wild type (36 genes up, 46 genes down) **(Fig. 6E, F)**. A comparison of all the differentially expressed genes containing both up and down genes is shown in the Venn diagram **(Fig. 6G).**

3.9 Differentially expressed genes in AD brain were overlapped with Aβ + tau *C. elegans* co-expression model

We compared our differential expressed genes list to previously published RNA-seq data from human AD brain (Twine et al., 2011)(**Table 3**). We confirmed an overlap of 8 genes: patched homolog 1, PTCH1 (*ptc-3*), the Rab GTPase activating protein, TBC1D16 (*tbc-16*), the WD repeat and FYVE domain-containing protein 3, WDFY3 (*wdfy-3*), myosin IXA, ADP-ribosylation factor guanine nucleotide exchange factor 2, ARFGEF2 (*agef-1*), Early B-cell Factor, EBF1 (*unc-3*), D-amino-acid oxidase, DAO (*daao-1*), glutamate receptor, metabotropic 1, GRM1 (*mgl-2*), prolyl 4-hydroxylase subunit alpha 2, P4HA2 (*dpy-18* and *phy-2*).

Four of these genes (*ptc-3, wdfy-3, agef-1, mgl-2)* were selected for qRT-PCR validation due to regulation in at least 2 comparisons (**Supplementary Table 4**). The results from qRT-PCR were consistent with those obtained from RNA-seq.

3.10 Functional annotation and GO enrichment analysis of regulated genes

To uncover biological themes of genes regulated by Aβ, pro-aggregating tau and anti-aggregating tau, we utilized the DAVID functional annotation tool to annotate,

extract and then analyze statistical enrichment for Gene ontology (**Fig. 7**). Eight categories were identified in the up-regulated gene list of comparisons of N2 vs UM0001 (Aβ+pro-aggregating tau). The most significant category in the up-regulated gene list is UDP-GlucuronosylTransferase (UGT) (*P*<7.40E-03). There are five genes (*ugt-31, ugt-32, ugt-25, ugt-29, ugt-63*), which are the orthologs of the phase II human transporter gene UGT3A2 (UDP-glycosyltransferase family 3 member A2) and UGT3A1 (UDP-glycosyltransferase family 3 member A1). Five genes involved in aging process were uncovered during the annotation *dod-23, lys-7, thn-1, sod-3, arch-1* (*P*<8.1E-2). GO analysis also revealed 5 genes (F26A1.4, K09C6.2, Y38H8A.3, Y39G8C.2, Y4C6A.1) presented in the protein phosphorylation (*P*<2.60E-02) category. We did not observe aging and protein phosphorylation categories in any of the comparisons between N2 and single transgenic strains.

In the down-regulated gene list of N2 vs UM0001 (Aβ + pro-aggregating tau), nematode cuticle collagen (36 genes, *P*<1.5E-21), structural constituent of cuticle (36 genes, *P*<1.4E-19), positive regulation of multicellular organism growth (48 genes, *P*<1.20E-10), metabolic process (65 genes, *P*<1.9E-8), peroxisome (11 genes, *P*<4.50E-07), EGF-like, conserved site (15 genes, *P*<2.40E-06) categories were observed to be overrepresented.

3.11 RNA interference reveals genetic enhancers and supressors of Aβ and aggregating tau transgenes

In order to evaluate the genetic interaction between most up-regulated genes and the human transgenes Aβ and tau in C. *elegans*. We tested the alteration of egg laying, lifespan and learning capacity. The RNAi clones were obtained from RNAi library (Source BioScience LifeSciences) and clones were available for 13 out of top 20 regulated genes. The transcript ID, gene name, human ortholog if known, and full description of these genes is shown in **Supplementary Table 5.** The result is shown in the **Table 4**. We found that knockdown of C53B7.7 (*nep-4*) expression could impair serotonin and levamisole sensitivity in the presence of Aβ and tau (P<0.001). In

contrast, knockdown of Y39G8C.2 (TTBK2) could enhance serotonin and levamisole sensitivity (P<0.001). The lifespan of C45G7.3 (RNAi) and three members (*fbxa-122, fbxa-124 and fbxa-125*) of the F-box gene family animals was significantly shorter than empty vector animals (P<0.0001). However, TTBK2 (RNAi) was found to live significantly longer (P<0.0001). The associative learning capacity of three members (*fbxa-122, fbxa-124 and fbxa-125*) of the F-box gene family (RNAi animals) and *nep-4* (RNAi) were worse than empty vector (RNAi). However, the chemotaxis index of TTBK2 (RNAi) animals was significantly higher than empty vector (RNAi) (*P*<0.0001).

4 Discussion

In this study, we generated and characterized a novel *C. elegans* model of AD by crossing two existing transgenic strains, each expressing human Aβ and tau, respectively in pan-neuronal cells. Using this model, we tested the hypothesis that the double transgenic model would have different phenotypes than the single transgene and thus provide new insights into the neurobiology of AD.

Previous studies have demonstrated that oxidative stress and cellular longevity play important roles in the pathogenesis of AD. *In vitro* experiments using primary central nervous system cultures demonstrated that Aβ treatment could increase the levels of H_2O_2 and lipid peroxides (Behl et al., 1994). These findings raise the question of whether the Aβ and tau-mediated proteotoxicity are associated with aging. Our results using a lifespan assay showed that co-expression of both Aβ and tau could shorten the lifespan of a double transgenic *C. elegans* model, indicating that Aβ and tau may trigger loss of proteostasis and apoptosis and thus cause the death of animals. The double transgenic animal lived significantly shorter than the two single transgene animals suggesting that both genes play a role in diminishing lifespan.

During the course of human AD, synaptic plasticity is altered, and many of the mechanisms involved in normal plasticity become dysregulated, leading to synapse dysfunction and collapse (Spires et al., 2014). Biochemical investigations of tissues from biopsy and autopsy indicate that various neurotransmitters and modulators

including acetylcholine (ACh), serotonin, and dopamine are differentially altered in the brains of individuals with AD (Kar et al., 2004). Human studies showed that the loss of serotonin (58%) receptor binding was found in the hippocampi of eight AD patients using autoradiography (Jansen et al., 1990). The decrease of DA could increase hypo-activity, cause gait disturbances and contribute to decline of executive functions and the occurrence of apathy (Robert et al., 2010). In clinical AD diagnoses, all behaviors as mentioned above are considered negative prognostic signs (Koch et al., 2013). Moreover, it has been shown that cholinergic receptors nAChR and mAChR mRNAs were differentially regulated within individual cholinergic neurons harvested from subjects diagnosed *ante mortem* as having no cognitive impairment (NCI), mild cognitive impairment (MCI), or mild to moderate AD, suggesting that cholinergic deficits occur during the progression of AD (Counts et al., 2007). In the light of these studies, we further investigated these neurotransmission pathways via behavioral assays. We found anti-aggregating tau did not cause behavioral deficits but pro-aggregating tau severely impaired serotoninergic and cholinergic signaling with or without the presence of Aβ, which suggests that tau-mediated neurotoxicity requires aggregation. These findings support previous concepts that tau belongs to the class of amyloidogenic proteins that share a common toxicity-mediating mechanism (Flach et al., 2012). Also, we found there was no significant difference between N2 (wild type) and CL2355 (Aβ strain), as well as BR5270 (pro-aggregating tau strain) and UM0001 (Aβ + pro-aggregating tau strain), indicating neuronal Aβ aggregates interfere with neurotransmitter signaling pathways, particularly the serotonergic pathway.

In the presence of pro-aggregating tau, Aβ slightly impaired cholinergic but not serotoninergic signaling, which suggests that tau aggregates may play a key role in synaptic transmission. Kraemer and coworkers (Kraemer et al., 2003) found similar results regarding the presynaptic defects due to the toxicity of abnormal tau aggregates in the worm model. Dopaminergic signaling undergoes several changes during the physiological aging process, but the involvement of dopamine system in

AD is still under debate (Portet et al., 2009; Attems et al., 2007). Our results of basal slowing response assay showed that co-expression of Aβ and tau could impair dopaminergic signaling, suggesting tau may interact with Aβ to cause an aggravation of dopaminergic dysfunction. Previous studies have demonstrated that Aβ can interfere with tau inducing conformational changes and neurodegeneration (Spires et al., 2014; Stancu et al., 2014).

An imbalance in cellular homeostasis may result in a decrease in brood size of *C. elegans* (Ewald et al., 2010; VanDuyn et al., 2010). It has been demonstrated that aggregates such as tau tangles and Aβ plaques may play a role in abnormalities in the *endosomal*-lysosomal pathway that occurs early in AD (Yoon et al., 2006), eventually leading to apoptotic cell death (Cacho-Valadez et al., 2012). A significant decrease in brood size of the double transgenic strain UM0001 (Aβ+pro-aggregate tau) was observed. Whether co-expression of Aβ and tau aggregates in the pan-neuron could interfere with *C. elegans* reproduction via the endosomal-lysosomal system would require further investigation. The most visible symptoms of Alzheimer's disease are memory loss and cognitive impairment. Therefore, memory is a critical criterion to assess the model. Not surprisingly, the double transgenic animals co-expressing Aβ and tau aggregates showed significant impairment in the butanone associative learning assay. Double transgenic animals were impaired at the level of Aβ single transgenic animals suggesting that expression of Aβ is the dominant transgene mediating this effect. A similar conclusion has been drawn from mouse AD models (Chiba et al., 2009; Ashe, 2001).

We were also able to show increased protein aggregation in the double transgenic Aβ + pro-aggregating tau strain using Congo red staining **(Fig.3)**. As we detected only modest aggregation in the pro-aggregating strain only, it appears likely that some interaction between the two transgenes can increase aggregation. Consistant with this result we also observed degeneration of dopamninergic neurons and punctate expression pattern in neuronal processes **(Fig.4).** Taken together, these results suggest that deficits observed in the behavioral assays could arise from

neuronal damage to specific neurons.

We also investigated gene expression profiles, since none of the previously published studies have described the relationship between AD worm model and human patients at the transcriptional level. We employed RNA-seq to reveal genes involved in AD. Gene expression changes resulting from Aβ aggregation and/or tau aggregation have been monitored by RNA-seq for almost all known or predicted *C. elegans* genes. Based on different hypotheses, we compared the gene expression changes to each group and generated up- and down- regulated gene lists using rigorous statistical criteria. To investigate whether genes identified in this model system also show gene expression changes in AD brain, we also matched our significant gene lists with a human RNA-seq study performed on AD total brain (Twine et al., 2011). An overlap of 8 genes was identified (**Table 3**).

The gene with the highest correlation, PTCH1, is a transmembrane protein involved in the abnormal loss of glial precursor cells and a cognition decline in Alzheimer's brains (He et al., 2014). The overexpression of PTCH1 in neural precursor cells was linked to aggregation of Aβ (Trazzi et al., 2011). The secondary 2 closely related genes are D-Amino acid oxidase (DAO) and prolyl 4-hydroxylase subunit alpha 2 (P4HA2). DAO encoding a D-serine degrading enzyme was reported to cooperate with glutamate to link neuroinflammation with excitotoxicity and P4HA2 encodes a component of prolyl 4-hydroxylase, a key enzyme in collagen synthesis composed of two identical alpha subunits and two beta subunits. This finding could help to explain the poor progeny viability of double transgenic animals. There are 2 orthologs of P4HA2 in *C. elegans dpy-18* and *phy-2*, which are essential for the survival of worms and embryonic development (Friedman et al., 2000). We also observed the down-regulation of ARFGEF2 gene in both worm AD model and human AD sample. ARFGEF2 encodes ADP-ribosylation factor guanine nucleotide exchange factor 2. Clinical reports demonstrated a child with ARFGEF2 mutations showed a severe choreadystonic movement disorder, bilateral periventricular nodular heterotopia (deWit et al., 2009). While performing basal slowing response assay, we observed

similar severe movement disorders in UM0001 (Aβ + pro-aggregating tau) strain (data not shown), suggesting that the neuroprotective role of ARFGEF2 may be conserved from nematode to human. A considerable age-dependent increase in cortical expression of Glutamate receptor, metabotropic 1 (GRM1) in a mouse model of AD was previously observed. Moreover, exposure of cortical neuronal cultures to β-amyloid oligomers upregulated mGluR1 cleavage. Taken together, increased levels of Aβ may trigger the overexpression of GRM1 that affect neuronal toxicity (Ostapchenko et al., 2013). It has been reported previously that WD repeat and FYVE domain-containing protein 3 (WDFY3; also known as the adaptor protein autophagy-linked FYVE protein, ALFY) has a central role in the autophagic degradation of aggregates and acts as a scaffold for aggregates, p62, and the autophagosome (Filimonenko et al., 2010). Both our worm model and the human study showed tau could decrease the expression of WDFY3, which may impair autophagy-lysosomal system suggesting that autophagic pathways could become possible therapeutic targets.

One limitation of this approach is that the age of *C. elegans* used for RNA-seq was larvae 4 (L4), since older animals have the confound of embryonic RNA. Comparing differences in L4 nematode RNA levels to Alzheimer's disease brain tissue RNAs may thus be highly speculative.

In the present study, five up-regulated UDP-GlucuronosylTransferases (UGT) (*ugt-31, ugt-32, ugt-25, ugt-29, ugt-63*) were detected. They are orthologs of the human gene UGT3A2 (UDP-glycosyltransferase family 3 member A2) and UGT3A1 (UDP-glycosyltransferase family 3 member A1). UGTs are well-known phase Ⅱ metabolic enzymes. Expression of UGTs can be increased as a general cellular response to increasing oxidative stress(Hasegawa et al., 2010) and aging (Murphy et al., 2003). It has been previously shown that the expression of *ugt-25* was up-regulated after ethosuximide treatment, which has neuroprotective activity on *C. elegans* model of tauopathy(Chen et al., 2015). Nonetheless, to our knowledge, no

reports have yet to demonstrate direct UGT, tau, and Aβ interaction.

We observed a large number of genes regulated in pro-aggregating tau animals (**Fig 6. C,D**). Because we also observed strong behavioral deficits in different assays (egg-laying, liffe-span, chemotaxis) in these animals, the results together suggests severe pathology due to this specific protein form. The small number of gene expression changes observed in anti-aggregating tau animals (Fig. 6. E,F) supports the notion that aggregation leads to the pathologic changes.

In the comparison of N2 vs UM0001 (Aβ + pro-aggregating tau), we also found one of the most up-regulated genes Y39G8C.2 (fold change 14.76, **Supplementary Table 2**) is an ortholog of human TTBK2 (tau tubulin kinase 2) and TTBK1 (tau tubulin kinase 1). TTBK2 and TTBK1 are up-regulated in AD brains and able to phosphorylate both tau and tubulin. They have been reported associated with late onset of AD (Ikezu &Ikezu, 2014; Houlden et al., 2007; Sato et al., 2006). In addition to tau and tubulin, TTBK1/2 has also been found to phosphorylate transactive response (TAR) DNA-binding protein 43, or TDP-43, a DNA/RNA binding protein responsible for transcriptional repression, pre-mRNA splicing, and translational regulation (Liachko et al., 2014). A group of researchers who have previously published a *C. elegans* tauopathies model (Kraemer et al., 2006) demonstrated that knockdown of TTBK1/2 could enhance the tau-induced UNC phenotype specifically.

To better link gene expression changes to genetic interactions, we performed RNAi of 13 genes available from the list of top 20 up-regulated genes in the wild type versus Aβ + pro-aggregating tau comparison. We uncovered 3 gene classes with interactions: F-box proteins family, Y39G8C.2 (TTBK2), and *nep-4*. The F-box A is a protein motif of approximately 50 amino acids that functions as a site of protein-protein interaction. F-box proteins were first characterized as components of SCF ubiquitin-ligase complexes (named after their main components, Skp1, Cullin, and an F-box protein), in which they bind substrates for ubiquitin-mediated proteolysis (Papaevgeniou and Chondrogianni, 2014). There are 11 F-box proteins in

the completed Saccharomyces cerevisiae genome, 326 predicted in Caenorhabditis *elegans*, 22 in Drosophila, and at least 38 in humans (Kipreos and Pagano, 2000). F-box proteins have been discovered to function in a diverse array of processes including cell proliferation, cell growth, signal transduction, and cellular and animal survival (Jin et al., 2004). In our study, *fbxa-122*, *fbxa-124* and *fbxa-125* RNAi shorten the lifespan and impair learning capacity of the double transgenic animals expressing both Aβ and pro-aggregating tau, indicating that F-box protein may play a neuro-protective role in the pathogenesis of neurodegenerative disease.

Moreover, Y39G8C.2 (TTBK2) (RNAi) animals display a serotonin and levamisole hypersensitivity in egg laying assay, indicating that TTBK2 may act as a modulator of serotoninergic and cholinergic signaling pathways. TTBK2 (RNAi) animals also have longer lifespan and higher learning index than control animals, suggesting its neuro-toxic role in the pathogeneses of AD, which may represent an attractive target for therapeutic intervention especially in the improvement of cognitive function and lifespan extension.

The *nep-4* gene encodes a *C. elegans* homolog of the mammalian peptidase family neprilysin. It has been shown that neprilysin degrades the amyloid beta peptide whose abnormal misfolding and aggregation in neural tissue has been implicated as a cause of Alzheimer's disease. We observed the *nep-4* (RNAi) animals have egg laying defects, shorter lifespan, and a severe defect in olfactory plasticity. It has been shown that a reduction in NEP-4 would result in decrease of egg laying of Drosophila, indicating a evolutionarily conserved biologic function of *nep-4* (Sitnik et al., 2014). Neprilysin-deficient knockout mice show both Alzheimer's-like behavioral impairment and amyloid-beta deposition in the brain (Madani et al., 2006), providing strong evidence for the protein's association with the Alzheimer's disease process.

5 Conclusions

Our data showed that co-expression of Aβ and tau in a *C. elegans* model of AD produce significant number of dysregulated processes that recapitulate some key

pathological characteristics of human AD. Expression of both Aβ and aggregating tau together showed additive effects in some behaviors such as average lifespan, progeny viability, but not all. Furthermore, we observed the dysregulation of genes concordant with those found in human AD. Taken together, our findings establish new insights into the differences and similarities in the contributions of Aβ and tau together or alone in neurobiology of AD using an invertebrate model organism.

6 Acknowledgments

We thank the Chris Wong lab and members of the genomics and bioinformatics core for sequencing, and members of the Garry Wong lab for comments and suggestions. NGS data analysis was performed in part at the high performance computing cluster (HPCC) which is supported by the Information and Communication Technology Office (ICTO) of the University of Macau. Some strains were provided by the CGC, which is funded by NIH Office of Research Infrastructure Programs (P40 OD010440). This study was supported by a University of Macau grant MYRG2015-00231-FHS.

7 References

Alexander, A. G., Marfil, V., &Li, C. (2014). Use of Caenorhabditis elegans as a model to study Alzheimer's disease and other neurodegenerative diseases, *5*(September), 1–21. http://doi.org/10.3389/fgene.2014.00279

Ardiel, E. L., &Rankin, C. H. (2010). An elegant mind: learning and memory in Caenorhabditis elegans. *Learning & Memory (Cold Spring Harbor, N.Y.)*, *17*(604), 191–201. http://doi.org/10.1101/lm.960510

Ashe, K. H. (2001). Learning and Memory in Transgenic Mice Modeling Alzheimer ' s Disease. *Learning & Memory*. http://doi.org/10.1101/lm.43701.of

Attems, J., Quass, M., &Jellinger, K. A. (2007). Tau and alpha-synuclein brainstem pathology in Alzheimer disease: relation with extrapyramidal signs. *Acta Neuropathologica*, *113*(1), 53–62. http://doi.org/10.1007/s00401-006-0146-9

Ballard, C., Gauthier, S., Corbett, A., Brayne, C., Aarsland, D., &Jones, E. (2011). Alzheimer's disease. *Lancet*, *377*(9770), 1019–31. http://doi.org/10.1016/S0140-6736(10)61349-9

Behl, C. (1994). Hydrogen peroxide mediates amyloid β protein toxicity. *Cell*, *77*(6), 817–827. http://doi.org/10.1016/0092-8674(94)90131-7

Bolmont, T., Clavaguera, F., Meyer-Luehmann, M., Herzig, M. C., Radde, R., Staufenbiel, M., …Jucker, M. (2007). Induction of Tau Pathology by Intracerebral Infusion of Amyloid-β-Containing Brain Extract and by Amyloid-β Deposition in APP × Tau Transgenic Mice. *The American Journal of Pathology*, *171*(6), 2012–2020. http://doi.org/10.2353/ajpath.2007.070403

Brandt, R., Gergou, A., Wacker, I., Fath, T., &Hutter, H. (2009). A Caenorhabditis elegans model of tau hyperphosphorylation: Induction of developmental defects by transgenic overexpression of Alzheimer's disease-like modified tau. *Neurobiology of Aging*, *30*, 22–33. http://doi.org/10.1016/j.neurobiolaging.2007.05.011

Brenner, S. (1974). The genetics of Caenorhabditis elegans. *Genetics*, *77*(1), 71–94. Retrieved from

http://www.pubmedcentral.nih.gov/articlerender.fcgi?artid=1213120&tool=pmcentrez&rendertype=abstract

Cacho-Valadez, B., Muñoz-Lobato, F., Pedrajas, J. R., Cabello, J., Fierro-González, J. C., Navas, P., …Miranda-Vizuete, A. (2012). Mitochondrial Thioredoxin System Uncovers an Unexpected Protective Role of Thioredoxin Reductase 2 in β-Amyloid Peptide Toxicity. *Antioxidants & Redox Signaling*, *16*(12), 1384–1400. http://doi.org/10.1089/ars.2011.4265

Chen, X., McCueF, H.V, Wong, S. Q., Kashyap, S. S., Kraemer, B. C., Barclay, J. W., …Morgan, A. (2015). Ethosuximide ameliorates neurodegenerative disease phenotypes by modulating DAF-16/FOXO target gene expression. *Molecular Neurodegeneration*, *10*(1), 51. http://doi.org/10.1186/s13024-015-0046-3

Chiba, T., Yamada, M., Sasabe, J., Terashita, K., Shimoda, M., Matsuoka, M., &Aiso, S. (2009). Amyloid-beta causes memory impairment by disturbing the JAK2/STAT3 axis in hippocampal neurons. *Mol Psychiatry*, *14*(2), 206–222. http://doi.org/10.1038/mp.2008.105

Counts, S. E., He, B., Che, S., Ikonomovic, M. D., DeKosky, S. T., Ginsberg, S. D., &Mufson, E. J. (2007). α7 Nicotinic Receptor Up-regulation in Cholinergic Basal Forebrain Neurons in Alzheimer Disease. *Archives of Neurology*, *64*(12), 1771. http://doi.org/10.1001/archneur.64.12.1771

deWit, M. C. Y., deCoo, I. F. M., Halley, D. J. J., Lequin, M. H., &Mancini, G. M. S. (2009). Movement disorder and neuronal migration disorder due to ARFGEF2 mutation. *Neurogenetics*, *10*(4), 333–6. http://doi.org/10.1007/s10048-009-0192-2

Dosanjh, L. E., Brown, M. K., Rao, G., Link, C. D., &Luo, Y. (2010). Behavioral phenotyping of a transgenic caenorhabditis elegans expressing neuronal amyloid-β *Journal of Alzheimer's Disease*, *19*, 681–690. http://doi.org/10.3233/JAD-2010-1267

Dostal, V., Roberts, C. M., &Link, C. D. (2010). Genetic mechanisms of coffee extract protection in a Caenorhabditis elegans model of β-amyloid peptide toxicity.

Genetics, *186*, 857–866. http://doi.org/10.1534/genetics.110.120436

Ewald, C. Y., &Li, C. (2010). Understanding the molecular basis of Alzheimer's disease using a Caenorhabditis elegans model system. *Brain Structure & Function*, *214*(2–3), 263–83. http://doi.org/10.1007/s00429-009-0235-3

F. He. (2011). *Lifespan Assay —BIO-PROTOCOL*. Retrieved from http://www.bio-protocol.org/e57

Fatouros, C., Pir, G. J., Biernat, J., Koushika, S. P., Mandelkow, E., Mandelkow, E. M., …Baumeister, R. (2012). Inhibition of Tau aggregation in a novel caenorhabditis elegans model of tauopathy mitigates proteotoxicity. *Human Molecular Genetics*, *21*, 3587–3603. http://doi.org/10.1093/hmg/dds190

Filimonenko, M., Isakson, P., Finley, K. D., Anderson, M., Jeong, H., Melia, T. J., …Yamamoto, A. (2010). The selective macroautophagic degradation of aggregated proteins requires the PI3P-binding protein Alfy. *Molecular Cell*, *38*(2), 265–79. http://doi.org/10.1016/j.molcel.2010.04.007

Flach, K., Hilbrich, I., Schiffmann, A., Gärtner, U., Krüger, M., Leonhardt, M., …Holzer, M. (2012). Tau oligomers impair artificial membrane integrity and cellular viability. *The Journal of Biological Chemistry*, *287*(52), 43223–33. http://doi.org/10.1074/jbc.M112.396176

Foster, N. L., Wilhelmsen, K., Sima, A. A., Jones, M. Z., D'Amato, C. J., &Gilman, S. (1997). Frontotemporal dementia and parkinsonism linked to chromosome 17: a consensus conference. Conference Participants. *Annals of Neurology*, *41*(6), 706–15. http://doi.org/10.1002/ana.410410606

Friedman, L., Higgin, J. J., Moulder, G., Barstead, R., Raines, R. T., &Kimble, J. (2000). Prolyl 4-hydroxylase is required for viability and morphogenesis in Caenorhabditis elegans. *Proceedings of the National Academy of Sciences of the United States of America*, *97*(9), 4736–41. Retrieved from http://www.ncbi.nlm.nih.gov/pubmed/10781079

Goate, A., Chartier-Harlin, M. C., Mullan, M., Brown, J., Crawford, F., Fidani, L., …James, L. (1991). Segregation of a missense mutation in the amyloid

precursor protein gene with familial Alzheimer's disease. *Nature*, *349*(6311), 704–6. http://doi.org/10.1038/349704a0

Hasegawa, K., Miwa, S., Tsutsumiuchi, K., Miwa, J., &Ahringer, J. (2010). Allyl Isothiocyanate that Induces GST and UGT Expression Confers Oxidative Stress Resistance on C. elegans, as Demonstrated by Nematode Biosensor. *PLoS ONE*, *5*(2), e9267. http://doi.org/10.1371/journal.pone.0009267

He, P., Staufenbiel, M., Li, R., &Shen, Y. (2014). Deficiency of patched 1-induced Gli1 signal transduction results in astrogenesis in Swedish mutated APP transgenic mice. *Human Molecular Genetics*, *23*(24), 6512–27. http://doi.org/10.1093/hmg/ddu370

Houlden, H., Johnson, J., Gardner-Thorpe, C., Lashley, T., Hernandez, D., Worth, P., …Wood, N. W. (2007). Mutations in TTBK2, encoding a kinase implicated in tau phosphorylation, segregate with spinocerebellar ataxia type 11. *Nature Genetics*, *39*(12), 1434–1436. http://doi.org/10.1038/ng.2007.43

Huang, D. W., Sherman, B. T., &Lempicki, R. A. (2009a). Bioinformatics enrichment tools: paths toward the comprehensive functional analysis of large gene lists. *Nucleic Acids Research*, *37*(1), 1–13. http://doi.org/10.1093/nar/gkn923

Huang, D. W., Sherman, B. T., &Lempicki, R. A. (2009b). Systematic and integrative analysis of large gene lists using DAVID bioinformatics resources. *Nature Protocols*, *4*(1), 44–57. http://doi.org/10.1038/nprot.2008.211

Hutton, M., Lendon, C. L., Rizzu, P., Baker, M., Froelich, S., Houlden, H., …Heutink, P. (1998). Association of missense and 5'-splice-site mutations in tau with the inherited dementia FTDP-17. *Nature*, *393*(6686), 702–5. http://doi.org/10.1038/31508

Ikezu, S., &Ikezu, T. (2014). Tau-tubulin kinase. *Frontiers in Molecular Neuroscience*, *7*, 33. http://doi.org/10.3389/fnmol.2014.00033

Ittner, L. M., &Götz, J. (2011). Amyloid-β and tau--a toxic pas de deux in Alzheimer's disease. *Nature Reviews. Neuroscience*, *12*(2), 65–72. http://doi.org/10.1038/nrn2967

Jansen, K. L., Faull, R. L., Dragunow, M., &Synek, B. L. (1990). Alzheimer's disease: changes in hippocampal N-methyl-D-aspartate, quisqualate, neurotensin, adenosine, benzodiazepine, serotonin and opioid receptors--an autoradiographic study. *Neuroscience*, *39*(3), 613–27. Retrieved from http://www.ncbi.nlm.nih.gov/pubmed/1965859

Jin, J., Cardozo, T., Lovering, R. C., Elledge, S. J., Pagano, M., &Harper, J. W. (2004). Systematic analysis and nomenclature of mammalian F-box proteins. *Genes & Development*, *18*(21), 2573–80. http://doi.org/10.1101/gad.1255304

Kar, S., Slowikowski, S. P. M., Westaway, D., &Mount, H. T. J. (2004). Interactions between beta-amyloid and central cholinergic neurons: implications for Alzheimer's disease. *Journal of Psychiatry & Neuroscience : JPN*, *29*(6), 427–41. Retrieved from http://www.ncbi.nlm.nih.gov/pubmed/15644984

Kauffman, A., Parsons, L., Stein, G., Wills, A., Kaletsky, R., &Murphy, C. (2011). C. elegans positive butanone learning, short-term, and long-term associative memory assays. *Journal of Visualized Experiments : JoVE*, (49), e2490. http://doi.org/10.3791/2490

Kipreos, E. T., &Pagano, M. (2000). The F-box protein family. *Genome Biology*, *1*(5), REVIEWS3002. http://doi.org/10.1186/gb-2000-1-5-reviews3002

Koch, G., Belli, L., Giudice, T.Lo, Lorenzo, F.Di, Sancesario, G. M., Sorge, R., …Martorana, A. (2013). Frailty among Alzheimer's disease patients. *CNS & Neurological Disorders Drug Targets*, *12*(4), 507–11. Retrieved from http://www.ncbi.nlm.nih.gov/pubmed/23574166

Kraemer, B. C., Burgess, J. K., Chen, J. H., Thomas, J. H., &Schellenberg, G. D. (2006). Molecular pathways that influence human tau-induced pathology in Caenorhabditis elegans. *Human Molecular Genetics*, *15*(9), 1483–1496. http://doi.org/10.1093/hmg/ddl067

Kraemer, B. C., Zhang, B., Leverenz, J. B., Thomas, J. H., Trojanowski, J. Q., &Schellenberg, G. D. (2003). Neurodegeneration and defective neurotransmission in a Caenorhabditis elegans model of tauopathy.

Proceedings of the National Academy of Sciences of the United States of America, *100*(17), 9980–9985. http://doi.org/10.1073/pnas.1533448100

Lakso, M., Vartiainen, S., Moilanen, A.-M., Sirviö, J., Thomas, J. H., Nass, R., …Wong, G. (2003). Dopaminergic neuronal loss and motor deficits in Caenorhabditis elegans overexpressing human alpha-synuclein. *Journal of Neurochemistry*, *86*(1), 165–72. Retrieved from http://www.ncbi.nlm.nih.gov/pubmed/12807436

Larson, E. B., Shadlen, M.-F., Wang, L., McCormick, W. C., Bowen, J. D., Teri, L., &Kukull, W. A. (2004). Survival after initial diagnosis of Alzheimer disease. *Annals of Internal Medicine*, *140*(7), 501–9. Retrieved from http://www.ncbi.nlm.nih.gov/pubmed/15068977

Levy-Lahad, E., Wasco, W., Poorkaj, P., Romano, D., Oshima, J., Pettingell, W., …al., e. (1995). Candidate gene for the chromosome 1 familial Alzheimer's disease locus. *Science*, *269*(5226), 973–977. http://doi.org/10.1126/science.7638622

Lewis, J., Dickson, D. W., Lin, W. L., Chisholm, L., Corral, A., Jones, G., …McGowan, E. (2001). Enhanced neurofibrillary degeneration in transgenic mice expressing mutant tau and APP. *Science (New York, N.Y.)*, *293*(5534), 1487–91. http://doi.org/10.1126/science.1058189

Li, J., &Le, W. (2013). Modeling neurodegenerative diseases in Caenorhabditis elegans. *Experimental Neurology*, *250*, 94–103. http://doi.org/10.1016/j.expneurol.2013.09.024

Liachko, N. F., McMillan, P. J., Strovas, T. J., Loomis, E., Greenup, L., Murrell, J. R., …Kraemer, B. C. (2014). The Tau Tubulin Kinases TTBK1/2 Promote Accumulation of Pathological TDP-43. *PLoS Genetics*, *10*(12), e1004803. http://doi.org/10.1371/journal.pgen.1004803

Link, C. D. (1995). Expression of human beta-amyloid peptide in transgenic Caenorhabditis elegans. *Proceedings of the National Academy of Sciences of the United States of America*, *92*(20), 9368–72. Retrieved from http://www.pubmedcentral.nih.gov/articlerender.fcgi?artid=40986&tool=pmcentrez&rendertype=abstract

Livak, K. J., &Schmittgen, T. D. (2001). Analysis of relative gene expression data using real-time quantitative PCR and the 2^-ΔΔCT Method. *Methods*, *25*, 402–408. http://doi.org/10.1006/meth.2001.1262

Madani, R., Poirier, R., Wolfer, D. P., Welzl, H., Groscurth, P., Lipp, H.-P., …Mohajeri, M. H. (2006). Lack of neprilysin suffices to generate murine amyloid-like deposits in the brain and behavioral deficit in vivo. *Journal of Neuroscience Research*, *84*(8), 1871–1878. http://doi.org/10.1002/jnr.21074

Martorell, P., Bataller, E., Llopis, S., Gonzalez, N., Álvarez, B., Montón, F., …Genovés, S. (2013). A Cocoa Peptide Protects Caenorhabditis elegans from Oxidative Stress and β-Amyloid Peptide Toxicity. *PLoS ONE*, *8*(5). http://doi.org/10.1371/journal.pone.0063283

McColl, G., Roberts, B. R., Pukala, T. L., Kenche, V. B., Roberts, C. M., Link, C. D., …Cherny, R. a. (2012). Utility of an improved model of amyloid-beta ($A\beta_{1-42}$) toxicity in Caenorhabditis elegans for drug screening for Alzheimer's disease. *Molecular Neurodegeneration*, *7*(1), 57. http://doi.org/10.1186/1750-1326-7-57

Murphy, C. T., McCarroll, S. A., Bargmann, C. I., Fraser, A., Kamath, R. S., Ahringer, J., …Kenyon, C. (2003). Genes that act downstream of DAF-16 to influence the lifespan of Caenorhabditis elegans. *Nature*, *424*(6946), 277–283. http://doi.org/10.1038/nature01789

Ostapchenko, V. G., Beraldo, F. H., Guimarães, A. L. S., Mishra, S., Guzman, M., Fan, J., …Prado, M. A. M. (2013). Increased prion protein processing and expression of metabotropic glutamate receptor 1 in a mouse model of Alzheimer's disease. *Journal of Neurochemistry*, *127*(3), 415–25. http://doi.org/10.1111/jnc.12296

Papaevgeniou, N., &Chondrogianni, N. (2014). The ubiquitin proteasome system in Caenorhabditis elegans and its regulation. *Redox Biology*, *2*, 333–47. http://doi.org/10.1016/j.redox.2014.01.007

Portet, F., Scarmeas, N., Cosentino, S., Helzner, E. P., &Stern, Y. (2009). Extrapyramidal signs before and after diagnosis of incident Alzheimer disease in a prospective population study. *Archives of Neurology*, *66*(9), 1120–6.

http://doi.org/10.1001/archneurol.2009.196

Robert, P. H., Mulin, E., Malléa, P., &David, R. (2010). REVIEW: Apathy Diagnosis, Assessment, and Treatment in Alzheimer's Disease. *CNS Neuroscience & Therapeutics*, *16*(5), 263–271. http://doi.org/10.1111/j.1755-5949.2009.00132.x

Rudgalvyte, M., Peltonen, J., Lakso, M., Nass, R., &Wong, G. (2015). RNA-Seq Reveals AcuteManganese Exposure Increases Endoplasmic Reticulum Related and Lipocalin mRNAs in Caenorhabditis elegans. *Jjournal of Biochemical Molecular Toxicology*, *30*(2), 97–105. http://doi.org/10.1002/jbt

Sangha, J. S., Sun, X., Wally, O. S. D., Zhang, K., Ji, X., Wang, Z., …Zhang, J. (2012). Liuwei Dihuang (LWDH), a Traditional Chinese Medicinal Formula, Protects against β-Amyloid Toxicity in Transgenic Caenorhabditis elegans. *PLoS ONE*, *7*(8). http://doi.org/10.1371/journal.pone.0043990

Sato, S., Cerny, R. L., Buescher, J. L., &Ikezu, T. (2006). Tau-tubulin kinase 1 (TTBK1), a neuron-specific tau kinase candidate, is involved in tau phosphorylation and aggregation. *Journal of Neurochemistry*, *98*(5), 1573–1584. http://doi.org/10.1111/j.1471-4159.2006.04059.x

Sawin, E. R., Ranganathan, R., &Horvitz, H. R. (2000). C. elegans locomotory rate is modulated by the environment through a dopaminergic pathway and by experience through a serotonergic pathway. *Neuron*, *26*(3), 619–631. http://doi.org/10.1016/S0896-6273(00)81199-X

Schroeder, B. E., &Koo, E. H. (2005). To think or not to think: synaptic activity and Abeta release. *Neuron*, *48*(6), 873–5. http://doi.org/10.1016/j.neuron.2005.12.005

Sitnik, J. L., Francis, C., Hens, K., Huybrechts, R., Wolfner, M. F., &Callaerts, P. (2014). Neprilysins: an evolutionarily conserved family of metalloproteases that play important roles in reproduction in Drosophila. *Genetics*, *196*(3), 781–97. http://doi.org/10.1534/genetics.113.160945

Smialowska, A., &Baumeister, R. (2006). Presenilin function in Caenorhabditis

elegans. *Neuro-Degenerative Diseases*, *3*(4–5), 227–32. http://doi.org/10.1159/000095260

Sonani, R. R., &Singh, N. K. (2014). Phycoerythrin extends life span and health span of Caenorhabditis elegans. http://doi.org/10.1007/s11357-014-9717-1

Spires-Jones, T. L., &Hyman, B. T. (2014). The intersection of amyloid beta and tau at synapses in Alzheimer's disease. *Neuron*, *82*(4), 756–71. http://doi.org/10.1016/j.neuron.2014.05.004

St George-Hyslop, P., Haines, J., Rogaev, E., Mortilla, M., Vaula, G., Pericak-Vance, M., …Crapper McLachlan, D. (1992). Genetic evidence for a novel familial Alzheimer's disease locus on chromosome 14. *Nature Genetics*, *2*(4), 330–4. http://doi.org/10.1038/ng1292-330

Stancu, I.-C., Vasconcelos, B., Terwel, D., &Dewachter, I. (2014). Models of β-amyloid induced Tau-pathology: the long and "folded" road to understand the mechanism. *Molecular Neurodegeneration*, *9*(1), 51. http://doi.org/10.1186/1750-1326-9-51

Trapnell C; Pachter L; Salzberg SL. (2009). TopHat: discovering splice junctions with RNA-Seq. - PubMed - NCBI. Retrieved February25, 2016, from http://www.ncbi.nlm.nih.gov/pubmed/19289445

Trazzi, S., Mitrugno, V. M., Valli, E., Fuchs, C., Rizzi, S., Guidi, S., …Ciani, E. (2011). APP-dependent up-regulation of Ptch1 underlies proliferation impairment of neural precursors in Down syndrome. *Human Molecular Genetics*, *20*(8), 1560–1573. http://doi.org/10.1093/hmg/ddr033

Twine, N. A., Janitz, K., Wilkins, M. R., &Janitz, M. (2011). Whole transcriptome sequencing reveals gene expression and splicing differences in brain regions affected by Alzheimer's disease. *PloS One*, *6*(1), e16266. http://doi.org/10.1371/journal.pone.0016266

VanDuyn, N., Settivari, R., Wong, G., &Nass, R. (2010). SKN-1/Nrf2 inhibits dopamine neuron degeneration in a Caenorhabditis elegans model of methylmercury toxicity. *Toxicological Sciences*, *118*(2), 613–624.

http://doi.org/10.1093/toxsci/kfq285

Wu, Y., Wu, Z., Butko, P., Christen, Y., Lambert, M. P., Klein, W. L., …Luo, Y. (2006). Amyloid-beta-induced pathological behaviors are suppressed by Ginkgo biloba extract EGb 761 and ginkgolides in transgenic Caenorhabditis elegans. *The Journal of Neuroscience : The Official Journal of the Society for Neuroscience*, *26*(50), 13102–13113. http://doi.org/10.1523/JNEUROSCI.3448-06.2006

Xin, L., Yamujala, R., Wang, Y., Wang, H., Wu, W. H., Lawton, M. a., …Di, R. (2013). Acetylcholineestarase-Inhibiting Alkaloids from Lycoris radiata Delay Paralysis of Amyloid Beta-Expressing Transgenic C. elegans CL4176. *PLoS ONE*, *8*(5). http://doi.org/10.1371/journal.pone.0063874

Yoon, S., Choi, J., Yoon, J., Huh, J.-W., &Kim, D. (2006). Okadaic acid induces JNK activation, bim overexpression and mitochondrial dysfunction in cultured rat cortical neurons. *Neuroscience Letters*, *394*(3), 190–5. http://doi.org/10.1016/j.neulet.2005.10.034

Zhao, X.-L., Wang, W.-A., Tan, J.-X., Huang, J.-K., Zhang, X., Zhang, B.-Z., …Huang, F.-D. (2010). Expression of beta-amyloid induced age-dependent presynaptic and axonal changes in Drosophila. *The Journal of Neuroscience : The Official Journal of the Society for Neuroscience*, *30*(4), 1512–22. http://doi.org/10.1523/JNEUROSCI.3699-09.2010

Figure 1.

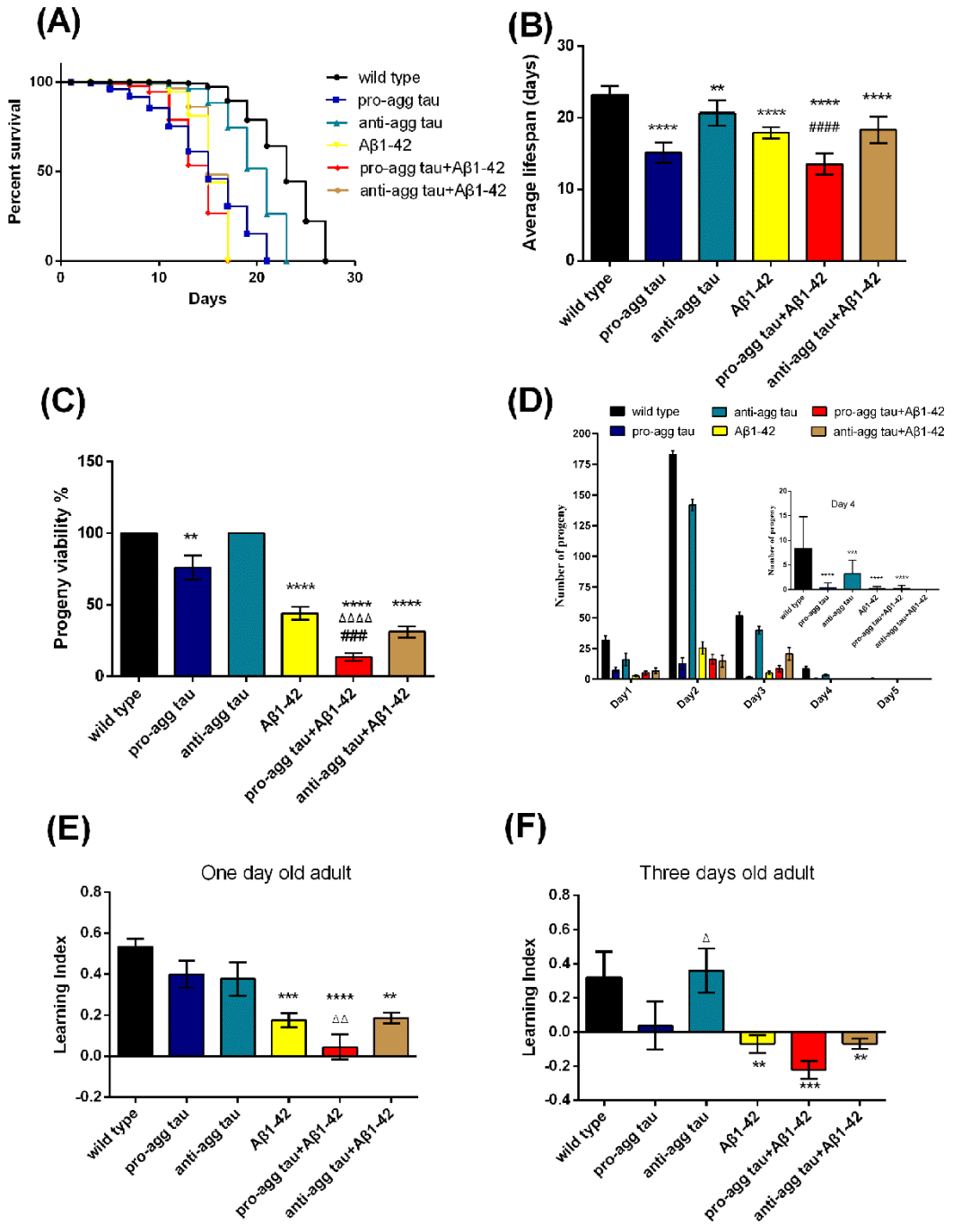

Figure 1. Life span, progeny viability and chemotaxis assays for wild type and transgenic strains. Strains used were: N2, wild type; BR5270, pro-aggregating tau; BR5271, anti-aggregating tau; CL2355, Aβ1-42; UM0001, pro-aggregating tau + Aβ1-42; UM0002, anti-aggregating tau + Aβ1-42. Significantly different from N2, ***P*<0.01, ****P*<0.001, *****P*<0.0001; significantly different from pro-aggregating tau, $^{\Delta\Delta}$*P*<0.01, $^{\Delta\Delta\Delta}$*P*<0.001, $^{\Delta\Delta\Delta\Delta}$*P*<0.0001; significantly different from Aβ1-42, $^{\#\#}$*P*<0.01, $^{\#\#\#}$*P*<0.001, $^{\#\#\#\#}$*P*<0.0001; One-way ANOVA, Tukey HSD post-hoc test. Error bars represent mean ± SEM. **(A)** Survival plot of wild type and transgenic strains. Fifty animals were counted for each strain as described in methods. **(B)** Average lifespan of wild type, single and

double transgenic animals, F(5,64)=12.85, *P*<0.0001. **(C)** Progeny viability was determined from eggs hatched within 1 day of laying in M9 buffer, n=24, F(5,65)=69.91, *P*<0.0001. **(D)** The reproductive lifespan of wild type, single and double transgenic animals. The insert figure represents eggs have been laid on the fourth day of adulthood, n=10. F (5, 54) = 13.25, *P*<0.0001. **(E)** and **(F)** Learning index was calculated from a butanone associative learning assay as described in methods. Error bar represent SEM, 3 replicates, 200-400 worms/replicate, $F(5,30)_{1\ day\ old}$=10.78, *P*<0.0001; $F\ (5, 12)_{3\ days\ old}$ = 14.44, *P*< 0.0001.

Figure 2.

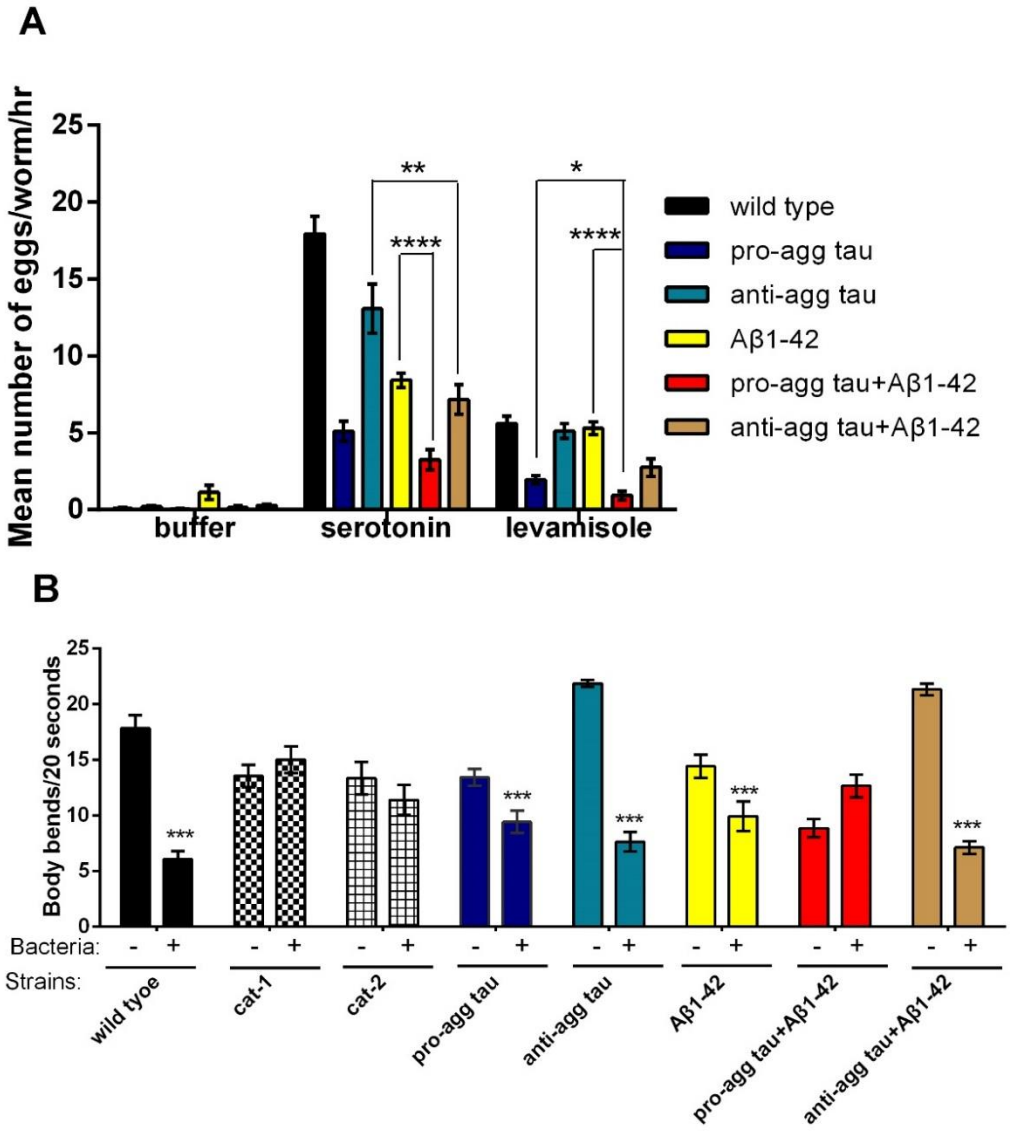

Figure 2. Egg laying and basal slowing response assay for wild type and transgenic strains. Strains used were: N2, wild type; BR5270, pro-aggregating tau; BR5271, anti-aggregating tau; CL2355, Aβ1-42; UM0001, pro-aggregating tau +Aβ1-42; UM0002, anti-aggregating tau +Aβ1-42. **(A)** Effects of serotonin (5 mg/mL) and levamisole (10 mg/mL) on egg laying in wild type and transgenic animals. Error bar represent the SEM from 32 animals. Statistical analysis was conducted using the One-way ANOVA, F(5,102) serotonin=67.21, *P*<0.0001; F(5,102) levamisole=30.72, *P*<0.0001. Tukey HSD post-hoc test. **P*<0.05, ***P*<0.01, ****P*<0.001, *****P*<0.0001. **(B)** Basal slowing response of wild type and transgenic animals. Body bends per 20 seconds were measured on NGM plates with or without bacteria as described in Methods. Thirty (30) young adult animals for each strain were scored. *cat-1* and *cat-2* served as control strains for loss of basal slowing response. Error bar represents the SEM. ****P*<0.001, student's t-test.

Figure 3.

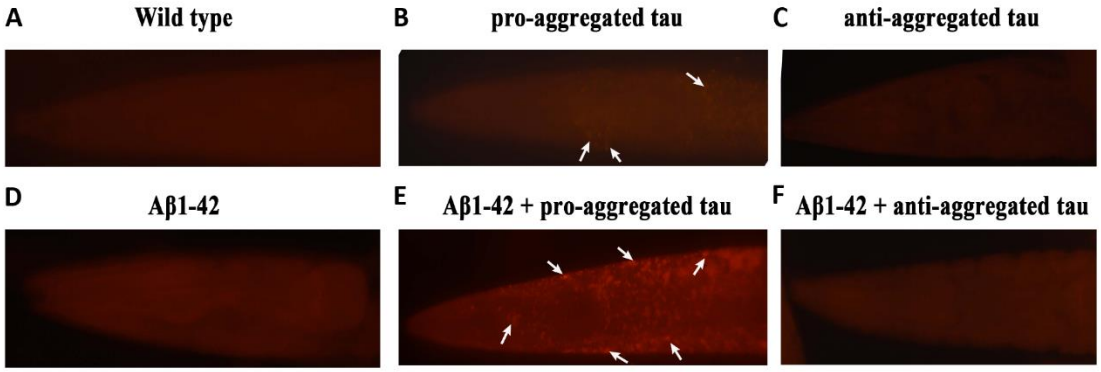

Figure 3. Congo red staining of wild type and transgenic animals. Animals were stained and viewed for protein aggregation in the head region anterior to the pharyngeal bulb. The strains are: **(A)** N2, wild type; **(B)**BR5270, pro-aggregating tau; **(C)**BR5271, anti-aggregating tau; **(D)**CL2355, Aβ1-42; **(E)** UM001, Aβ1-42 + pro-aggregating tau; **(F)** UM002, Aβ1-42 + anti-aggregating tau. Congo red stained deposits (white arrows) are visible in the head region of C. *elegans* expressing pro-aggregating tau and human Aβ1-42 + pro-aggregating tau as indicated. All Congo red staining experiments were performed twice with 50-100 animals of each strain.

Figure 4.

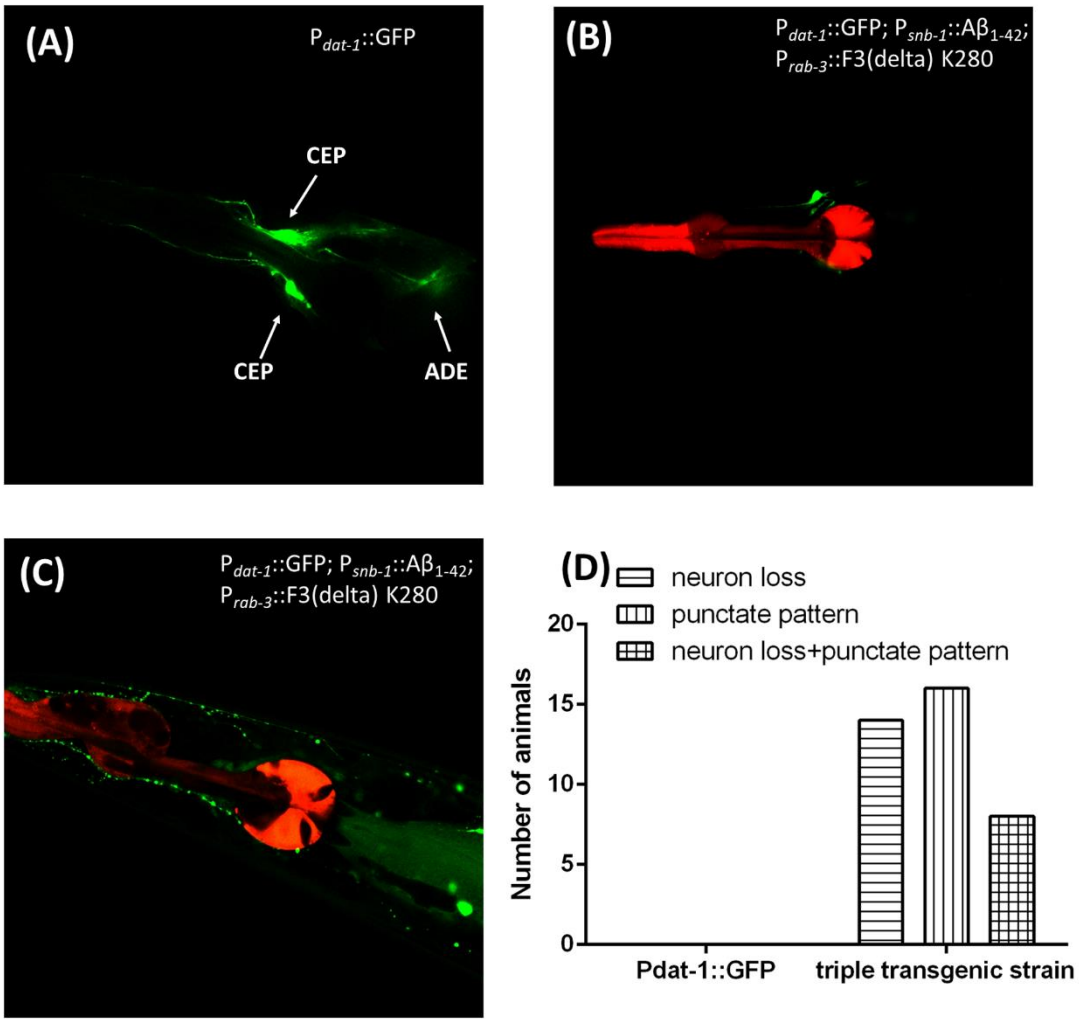

Figure 4. Confocal imaging of dopaminergic neurons and neuronal processes in adult C. *elegans.* Images were obtained using Zeiss confocal microscope LSM710 at 400X magnification. **(A)** Three-dimensional structure of confocal epifluorescence from head dopaminergic neurons in a P_{dat-1} : : GFP transgenic line. **(B)** The dopaminergic neurons were missing in triple transgenic strain (P_{dat-1}::GFP; P_{snb-1}::Aβ$_{1-42}$; P_{rab-3}::F3(delta) K280). **(C)** Animals expressing human Aβ and tau display a discontinuous punctate pattern in dopaminergic neurons. **(D)** The quantitative analysis of neurodegeneration. Thirty single transgenic (P_{dat-1} : : GFP) or triple transgenic animals (P_{dat-1}::GFP; P_{snb-1}::Aβ$_{1-42}$; P_{rab-3}::F3(delta) K280) were scored for neuronal loss or punctate neuronal process pattern.

Figure 5.

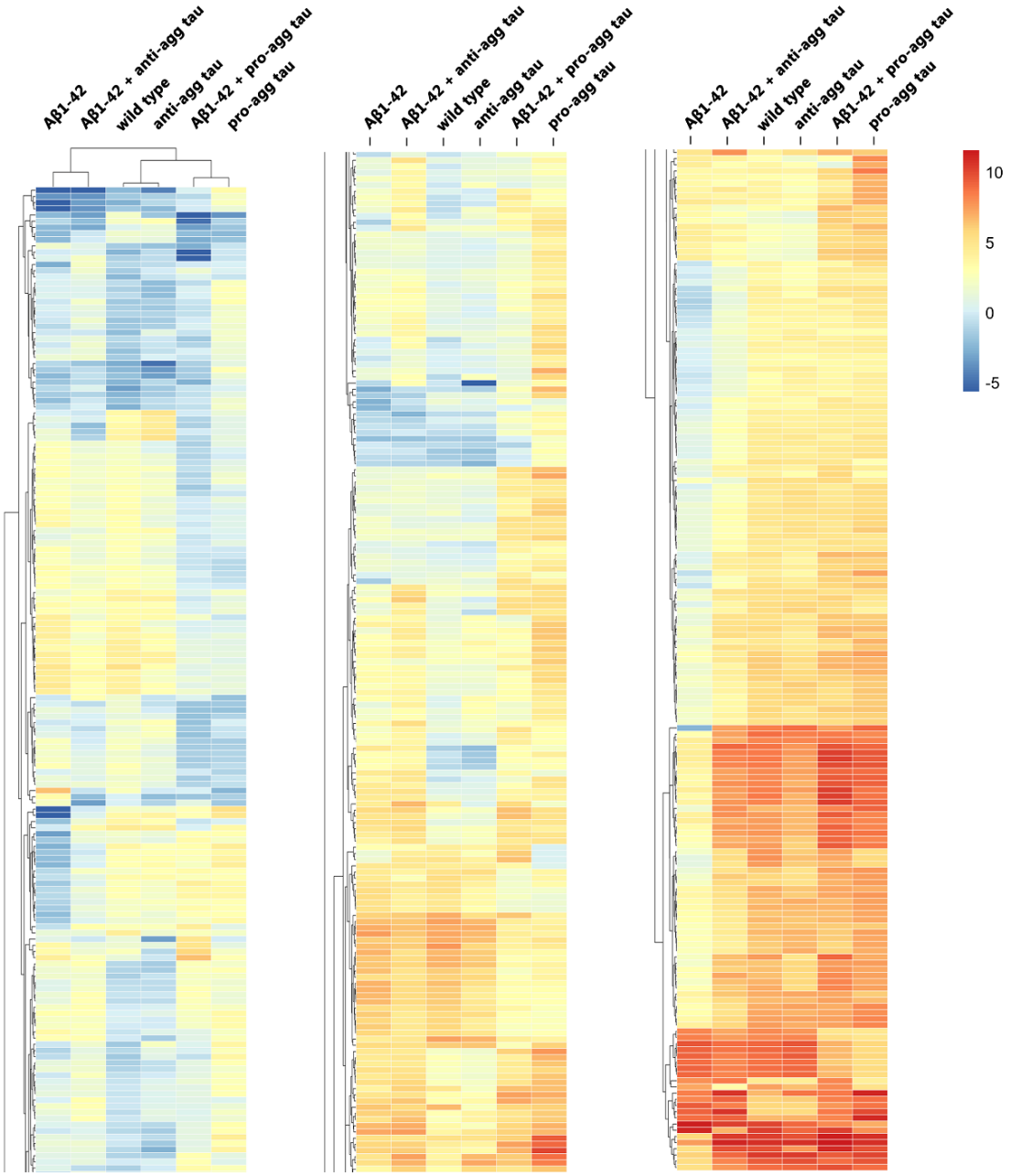

Figure 5. Hierarchical clustering diagram of genes expressed in wild type and transgenic Aβ1-42 and tau strains. Unsupervised hierarchical clustering of strains performed on average gene expression values using Euclidean distance. The distance between the nodes at the top scale indicates the similarity of gene expression between the groups calculated with Pearson's Correlation. Expression values of all genes are shown in logarithmic scale. The heat-map bar is shown on the right. Genes that were significantly different between strains (489 genes, $p<0.05$, 3 fold difference) were filtered and used for clustering.

Figure 6.

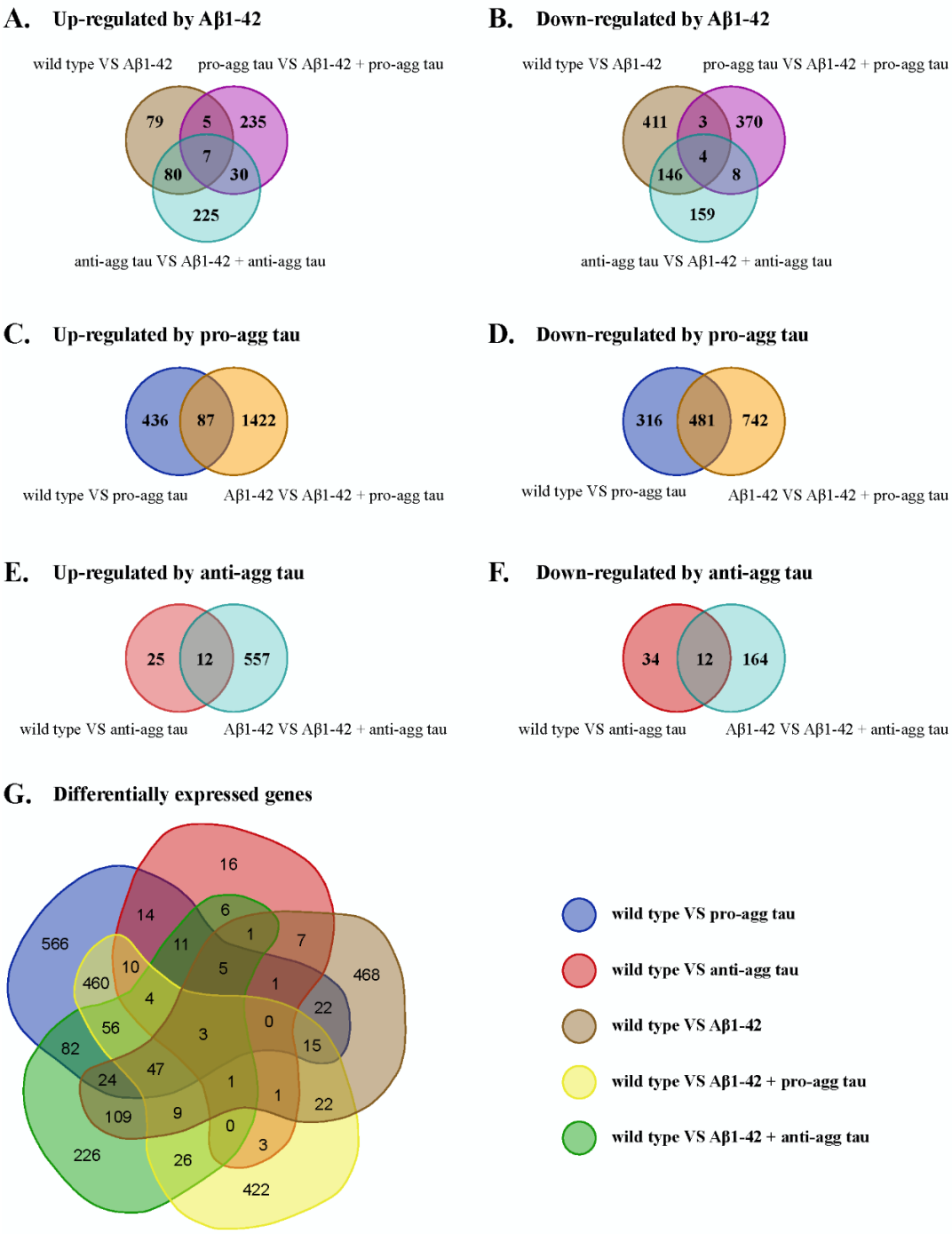

Figure 6. Venn diagram of genes significantly regulated between wild type, Aβ, and tau transgenic strains. Differentially expressed genes were obtained from cuffdiff as described in Methods. Differentially expressed genes that were up-regulated **(A)** or downregulated **(B)** in transgenic strains containing the Aβ transgene are shown. Differentially expressed genes that were up-regulated **(C, E)** or downregulated **(D, F)** in transgenic strains containing the pro-aggregating tau or anti-aggregating tau, respectively are shown as indicated. Venn diagram of five strains differentially expressed genes versus wild type (**G**).

Figure 7.

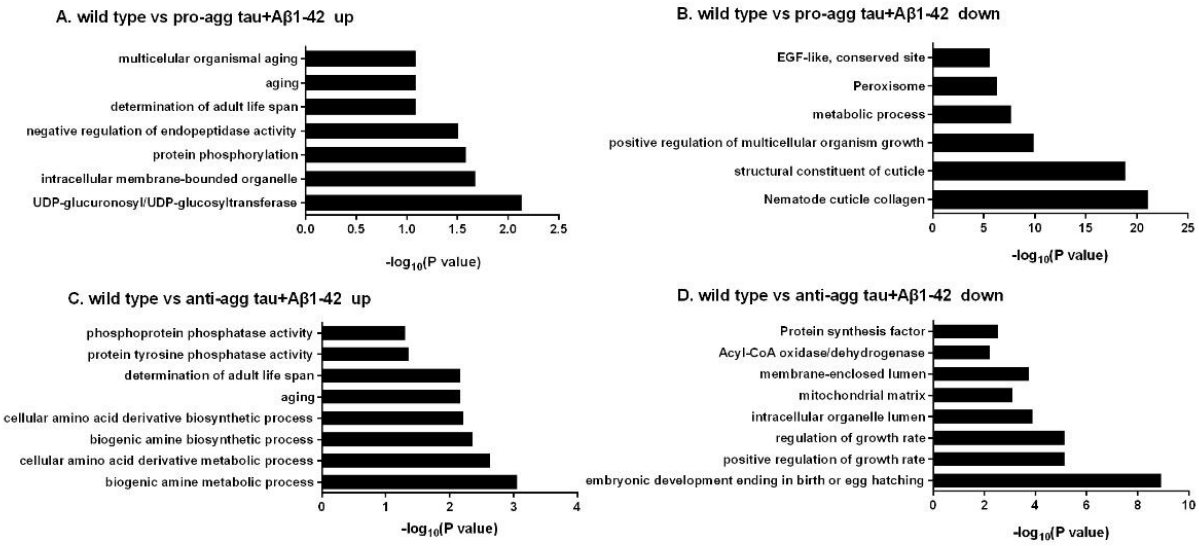

Figure 7. Gene ontology (GO) enrichment analysis of differentiall expressed genes between wild type and double transgenic strains. RNA-seq wild type vs pro-aggregating tau+ Aβ1-42 list of up-regulated genes (248 total) **(A)** or down-regulated (805 total) (**B)** was analyzed for GO category enrichment using DAVID 6.7 annotation tool as described in Methods. Bar indicates the level of significance. GO category enrichment from RNA-seq lists of genes up-regulated (293 total) **(C)** or down-regulted (295 genes) **(D)** in the comparison of wild type vs anti-aggregating tau+ Aβ1-42.

Table 1. Description of transgenic C. *elegans* strains used in this study

Associated protein	Strain	Transgene	Transgene expression	Phenotype
	N2	-	-	Wild type
Aβ peptide	CL2355	P_{snb-1}::$Aβ_{1-42}$	Inducible pan-neuronal	Deficits in chemotaxis, associative learning, and thrashing in liquid(Wu et al., 2006; Dosanjh et al., 2010)
Pro-aggregating tau	BR5270	P_{rab-3}::F3(delta)K280	Pan-neuronal	Uncoordinated movement, axonal defects, alterations in presynaptic cell(Fatouros et al., 2012)
Anti-aggregating tau	BR5271	P_{rab-3}::F3(delta)K280 I277P I380P	Pan-neuronal	Less morphological alteration and a milder phenotype
Vesicular monoamine transporters	*cat-1*	-	-	Defects in vesicle packaging of dopamine(Sawin, et al., 2000)
Putative tyrosine hydroxylase	*cat-2*	-	-	Defects in dopamine biosynthesis(Ardiel et al., 2010)
Aβ peptide and pro-aggregating tau	UM0001	P_{snb-1}::$Aβ_{1-42}$+P_{rab-3}:: F3(delta) K280	Inducible Pan-neuronal + pan-neuronal	This study
Aβ peptide and anti-aggregating tau	UM0002	P_{snb-1}::$Aβ_{1-42}$+P_{rab-3}:: F3(delta)K280 I277P I380P	Inducible Pan-neuronal + pan-neuronal	This study

Table 2. Thirty of the most regulated genes in N2 (wildtype) versus UM0001 (Pro-aggregated tau + $A\beta_{1-42}$)

Up-regulated genes			
Transcript ID	Gene name	$\log2(\frac{FPKM_{UM0001}}{FPKM_{N2}})$	q value
B0041.1	na	5.20	3.41E-03
C45G7.3	*ilys*-3	5.17	4.46E-02
F15D4.6	na	5.16	1.93E-03
Y37H2A.7	na	4.71	4.74E-02
C08F11.7	na	4.60	4.09E-02
T13A10.1	na	4.46	3.54E-02
M02E1.3	na	4.41	1.93E-03
Y53C10A.13	*fbxa*-122	4.37	1.93E-03
C53B7.7	*nep*-4	4.27	1.93E-03
K04G2.11	*scbp*-2	4.14	5.86E-03
F22D6.8	na	4.09	1.93E-03
T26C11.9	na	4.09	7.99E-03
R03H10.6	na	4.06	1.93E-03
T28A8.8	na	4.00	1.93E-03
F26G1.8	*msp-42*	3.99	1.93E-03

Down-regulated genes			
Transcript ID	Gene name	$\log2(\frac{FPKM_{UM0001}}{FPKM_{N2}})$	q value
T01D1.6	*abu*-11	-4.76	1.93E-03
K11D12.4	*cpt*-4	-4.74	1.93E-03
F28B4.3	na	-4.41	1.93E-03
F59B10.3	na	-4.40	3.44E-02
W01F3.3	*mtl*-11	-4.38	1.93E-03
R12E2.6	na	-4.24	3.12E-02
ZK662.2	na	-4.22	1.26E-02
C29F3.1	*ech*-1.1	-4.11	1.93E-03
Y71D11A.1	*edh*-12	-4.10	1.93E-03
Y43D4A.5	na	-3.98	1.93E-03
C49D10.4	*oac-10*	-3.95	8.96E-03
ZK682.5	*Iron-2*	-3.89	4.70E-03
ZK377.1	*wrt-6*	-3.89	1.93E-03
C34E11.2	na	-3.84	3.44E-02
C53B4.8	*mltn-12*	-3.83	1.93E-03

na: not available**.**

Table 3. Concordance of gene expression changes between C. *elegans* model and human AD brain.

Human Gene / C. *elegans* model	PTCH1	TBC1D16	WDFY3	ARFGEF2	EBF1	DAO	GRM1	P4HA2
N2 vs agg tau	-/-			-/-				+/-
Aβ vs (Aβ+ pro-agg tau)	-/-	-/-	-/-		-/-		-/-	+/-
N2 vs (Aβ+ pro-agg tau)	-/-		-/-	-/-			-/-	+/-
N2 vs (Aβ+ anti-agg tau)				-/-		-/+		

"+/+" represents this gene were up-regulated in both AD brain and worm samples
"-/-" represent this gene were down-regulated in both AD brain and worm samples
"+/-" represents this gene were up-regulated in AD brain but down-regulated in worm samples
"-/+" represents this gene were down-regulated in AD brain but up-regulated in worm samples

Table 4. RNA interference of 13 most up-regulated genes in UM0001 hAβ+pro-aggregating tau animals.

	Egg laying assay			Lifespan assay	Chemotaxis assay
	Buffer	Serotonin	Levamisole		
GENE	MEAN±SEM	MEAN±SEM	MEAN±SEM	Mean ±SEM	MEAN±SEM
Empty Vector	0.125±0.342	5.25±0.514	2.917±0.281	13.58±1.45	0.0531±0.0342
B0041.1	0.214±0.412	6.121±0.521	3.112±0.322	13.89±1.58	0.0417±0.0287
C45G7.3	0.114±0.234	4.179±0.417	2.325±0.194	9.25±1.34****	0.0569±0.0224
F15D4.6	0.178±0.297	5.198±0.359	2.565±0.215	12.36±1.28	0.0674±0.0364
Y37H2A.7	0.156±0.245	6.022±0.351	2.118±0.119	11.33±1.57	0.0754±0.0298
C08F11.7	0.117±0.215	4.658±0.287	2.568±0.289	12.51±1.21	0.0587±0.0354
T13A10.1	0.187±0.118	5.189±0.489	2.327±0.221	13.14±1.37	0.0546±0.0258
Pseudo Y53C10A.13 (*fbxa-122*)	0.114±0.158	5.05±1.623	2.451±0.341	8.14±1.58****	-0.256±0.0448****
C53B7.7 (*nep-4*)	0.141±0.356	0.142±0.224***	0.132±0.248****	8.21±1.14****	-0.387±0.0356***
R03H10.6	0.159±0.294	4.151±0.118	2.121±0.274	9.14±1.12****	-0.358±0.0298****
Pseudo Y53C10A.7(*fbxa-124*)	0.248±0.269	6.53±1.942	3.221±0.312	8.25±1.65****	-0.394±0.0341****
B0511.3 (*fbxa-125*)	0.287±0.187	5.579±1.542	3.114±0.412	9.29±1.87****	-0.257±0.0258****
Y39G8C.2 (TTBK2)	0.197±0.298	10.33±1.25***	5.298±0.421***	20.17±1.79****	0.326±0.0359****
K10C2.7	0.201±0.185	4.315±0.682	2.213±0.245	14.23±1.54	0.0369±0.0287

Significantly different from empty vector, ****P*<0.001, *****P*<0.0001

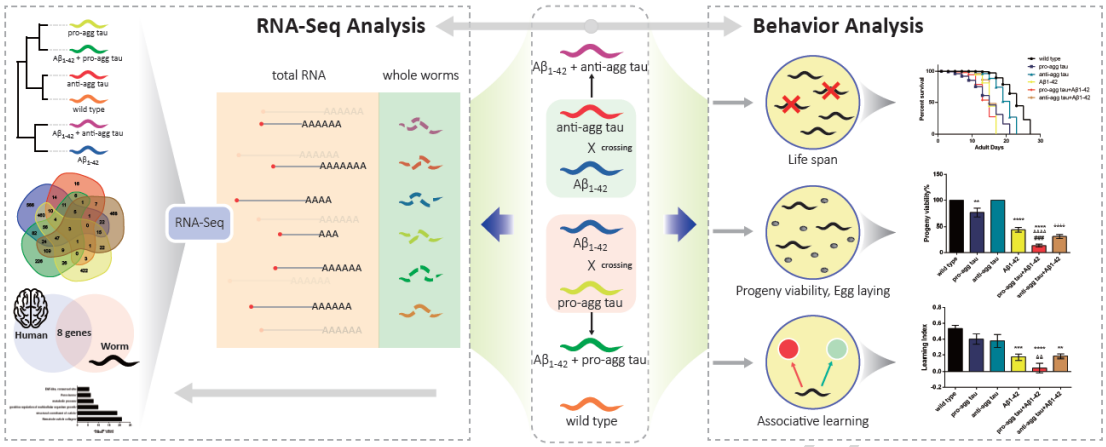

Graphical abstract

Highlights – Wang et al., 2017

- A transgenic *C. elegans* model co-expressing human Aβ1-42 and human tau has been established.
- Human Aβ1-42 and human tau co-expression shortens the life span of *C. elegans.*
- Human Aβ1-42 and human tau co-expression interferes with neurotransmitter signaling pathways, significantly decreases brood size, and disrupts chemotaxis associative learning.
- Eight differentially expressed genes in the *C. elegans* model overlapped with those differentially expressed in human AD brains.